Multi-modal skin atlas identifies a multicellular immune-stromal community associated with disrupted cornification and specific T cell expansion in atopic dermatitis

Evgenij Fiskin[1]*, Gökcen Eraslan[1]*§, Maria B. Alora-Palli[2]*, Tanvi Jain[1]*, Juan Manuel Leyva-Castillo[3], Sean Kim[4], Heather Choe[4], Caleb A. Lareau[5]§§, Helena Lau[4], Emily P. Finan[1], Isabella Teixeira-Soldano[1], Brenna LaBere[3,6], Anne Chu[3], Brian Woods[3], Janet Chou[3], Michal Slyper[1], Julia Waldman[1], Sabina Islam[7], Lynda Schneider[3], Wanda Phipatanakul[3], Craig Platt[3], Orit Rozenblatt-Rosen[1]§, Toni M. Delorey[1], Orr Ashenberg[1], Jacques Deguine[1], Gideon P. Smith[2], Raif S. Geha[3]‡, Aviv Regev[1,8]‡§, Ramnik Xavier[1,,4,9]‡

[1]Klarman Cell Observatory, Broad Institute of Harvard and MIT, Cambridge, MA, USA

[2]Department of Dermatology, Massachusetts General Hospital and Harvard Medical School, Boston, MA, USA

[3]Division of Immunology, Boston Children's Hospital, Harvard Medical School, Boston, MA, USA

[4]Center for Computational and Integrative Biology, Massachusetts General Hospital and Harvard Medical School, Boston, MA, USA

[5]Departments of Pathology, Stanford University, Stanford, CA, USA

[6]Division of Pulmonology, Section of Allergy-Immunology, Phoenix Children's Hospital, Phoenix, AZ, USA

[7]Center for Immunology and Inflammatory Diseases, Division of Rheumatology, Allergy and Immunology, Massachusetts General Hospital, Harvard Medical School, Boston, MA, USA

[8]Howard Hughes Medical Institute, Department of Biology, Massachusetts Institute of Technology, Cambridge, MA, USA

[9]Department of Molecular Biology, Massachusetts General Hospital and Harvard Medical School, Boston, MA, USA

* Contributed equally

‡ To whom correspondence should be addressed: raif.geha@childrens.harvard.edu, aviv.regev.sc@gmail.com, xavier@molbio.mgh.harvard.edu

§ Present address: Computational and Systems Biology Program, Memorial Sloan Kettering Cancer Center, New York, NY, USA

§§ Present address: Genentech, 1 DNA Way, South San Francisco, CA, USA

Supplementary Figures

	ID	Disease status	Sex	Age range	Global disease assessment	EASI	3' scRNA-seq Biopsy site lesional	3' scRNA-seq Biopsy site non-lesional	3' scRNA-seq Biopsy site healthy	5' scRNA-seq Biopsy site lesional	5' scRNA-seq Biopsy site non-lesional	Asthma
Hospital site A	BCH01	AD	M	25-30	2 - Mild	5.9	Antecubital fossa (L)	Inn arm (L)	—	—	—	Unknown
	BCH04	AD	F	20-25	4 - Severe	23.6	Upper back (L)	Lower back (R)	—	—	—	Unknown
	BCH05	AD	F	20-25	1 - Almost clear	0.7	Antecubital fossa (L)	Unknown	—	—	—	Unknown
	BCH06	AD	F	60-65	4 -Severe	36.6	Lower back	Unknown	—	—	—	Unknown
	BCH07	AD	M	25-30	2 - Mild	3.5	Arm (L)	Unknown	—	—	—	Unknown
	ECZ_1	AD	F	15-20	3 - Moderate	15	Unknown	Unknown	—	Arm (R)	Arm (R)	Unknown
	ECZ_3	AD	M	20-25	2 - Mild	1.4	Unknown	Unknown	—	Arm (R)	Arm (R)	Unknown
	ECZ_4	AD	M	20-25	2 - Mild	4	Unknown	Unknown	—	Arm (R)	Arm (R)	Unknown
	ECZ_5	AD	F	20-25	2 - Mild	3	Unknown	Unknown	—	Leg (L)	Leg (L)	Unknown
Hospital site B	MGH103	AD	M	Unknown	3- Moderate	Unknown	Lower leg (L)	Lower leg (L)	—	—	—	No
	MGH104	AD	M	Unknown	3- Moderate	Unknown	Back (R)	Back (R)	—	—	—	No
	MGH105	AD	F	Unknown	3- Moderate	Unknown	Thigh (R)	Thigh (R)	—	Unknown	—	Yes
	MGH106	AD	F	Unknown	2 - Mild	Unknown	Antecubital fossa (R)	Antecubital fossa (R)	—	Unknown	Unknown	No
	MGH108	AD	M	Unknown	3- Moderate	Unknown	Back (R)	Back (R)	—	—	—	No
	MGH110	AD	F	Unknown	4 - Severe	Unknown	Forearm (L)	Forearm (L)	—	—	—	Yes
	MGH114	AD	F	20-25	1 - Almost clear	Unknown	—	—	—	Forearm (R)	Forearm (R)	Unknown
	MGH117	AD	M	65-70	2 - Mild	Unknown	—	—	—	Upper arm (L)	Upper arm (L)	Unknown
	MGH101	Sclero	F	Unknown	3- Moderate	—	Chest (R)	Chest (R)	—	—	—	No
	MGH109	Sclero	F	Unknown	4 - Severe	—	Forearm (L)	Forearm (L)	—	—	—	No
	Healthy1	Healthy	F	Unknown	0 - Clear	—	—	—	Unknown	—	—	No
	Healthy2	Healthy	F	Unknown	0 - Clear	—	—	—	Unknown	—	—	No
	Healthy5	Healthy	F	Unknown	0 - Clear	—	—	—	Unknown	—	—	No
	Healthy6	Healthy	M	Unknown	0 - Clear	—	—	—	Unknown	—	—	No
	Healthy7	Healthy	M	Unknown	0 - Clear	—	—	—	Unknown	—	—	No
	Healthy8	Healthy	M	Unknown	0 - Clear	—	—	—	Unknown	—	—	No

Supplementary Figure 1. Patient cohort overview.

Patient demographics, assessed disease severity, biopsy locations and co-morbidities are noted. Unavailable information is noted as ‘Unknown’.

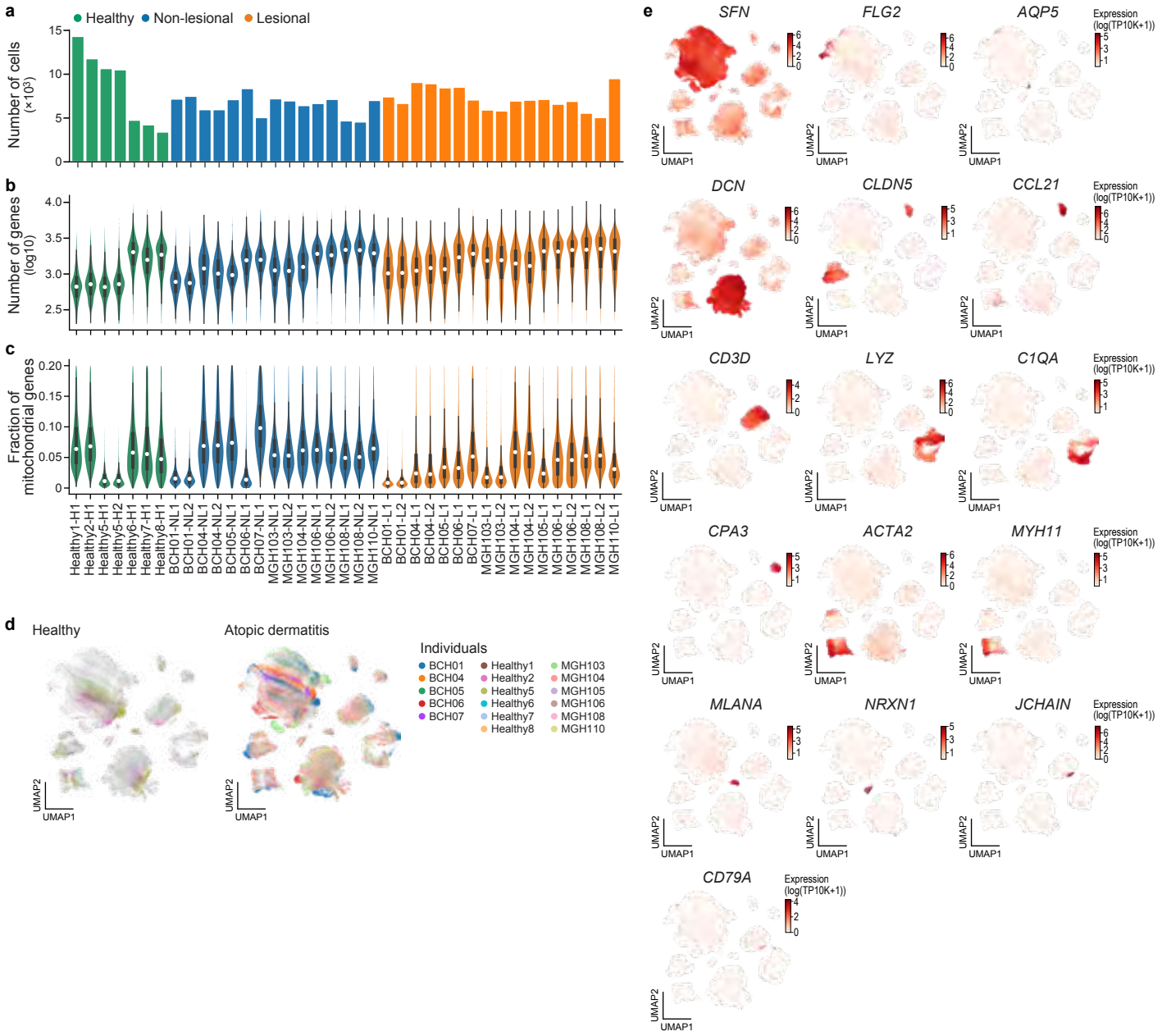
a
Healthy
Non-lesional
Lesional
Number of cells (×10³)
b
Number of genes (log10)
c
Fraction of mitochondrial genes
Healthy1-H1
Healthy2-H1
Healthy5-H1
Healthy5-H2
Healthy6-H1
Healthy7-H1
Healthy8-H1
BCH01-NL1
BCH01-NL2
BCH04-NL1
BCH04-NL2
BCH05-NL1
BCH06-NL1
BCH07-NL1
MGH103-NL1
MGH103-NL2
MGH104-NL1
MGH106-NL1
MGH106-NL2
MGH108-NL1
MGH108-NL2
MGH110-NL1
BCH01-L1
BCH01-L2
BCH04-L1
BCH04-L2
BCH05-L1
BCH06-L1
BCH07-L1
MGH103-L1
MGH103-L2
MGH104-L1
MGH104-L2
MGH105-L1
MGH106-L1
MGH106-L2
MGH108-L1
MGH108-L2
MGH110-L1
d
Healthy
Atopic dermatitis
UMAP1
UMAP2
Individuals
BCH01
BCH04
BCH05
BCH06
BCH07
Healthy1
Healthy2
Healthy5
Healthy6
Healthy7
Healthy8
MGH103
MGH104
MGH105
MGH106
MGH108
MGH110
e
SFN
FLG2
AQP5
DCN
CLDN5
CCL21
CD3D
LYZ
C1QA
CPA3
ACTA2
MYH11
MLANA
NRXN1
JCHAIN
CD79A
Expression (log(TP10K+1))

Supplementary Figure 2. Quality control of scRNA-seq skin cell atlas.

a-c, Quality metrics. Number of recovered cell barcodes passing quality control and filtering steps (a, y axis), distribution of the number of genes per cell barcode (b, y axis), and distribution of fraction of detected mitochondrial genes per cell barcode (c, y axis) in each processed channel (x axis) from healthy (green), non-lesional (blue) and lesional (orange) skin. White dots: median. **d,e**, Individual mixing and marker expression. 2D embedding of scRNA-seq profiles from the entire cohort colored by profiled individuals (d) or expression of coarse cell type markers (e, log(TP10K+1), color bar).

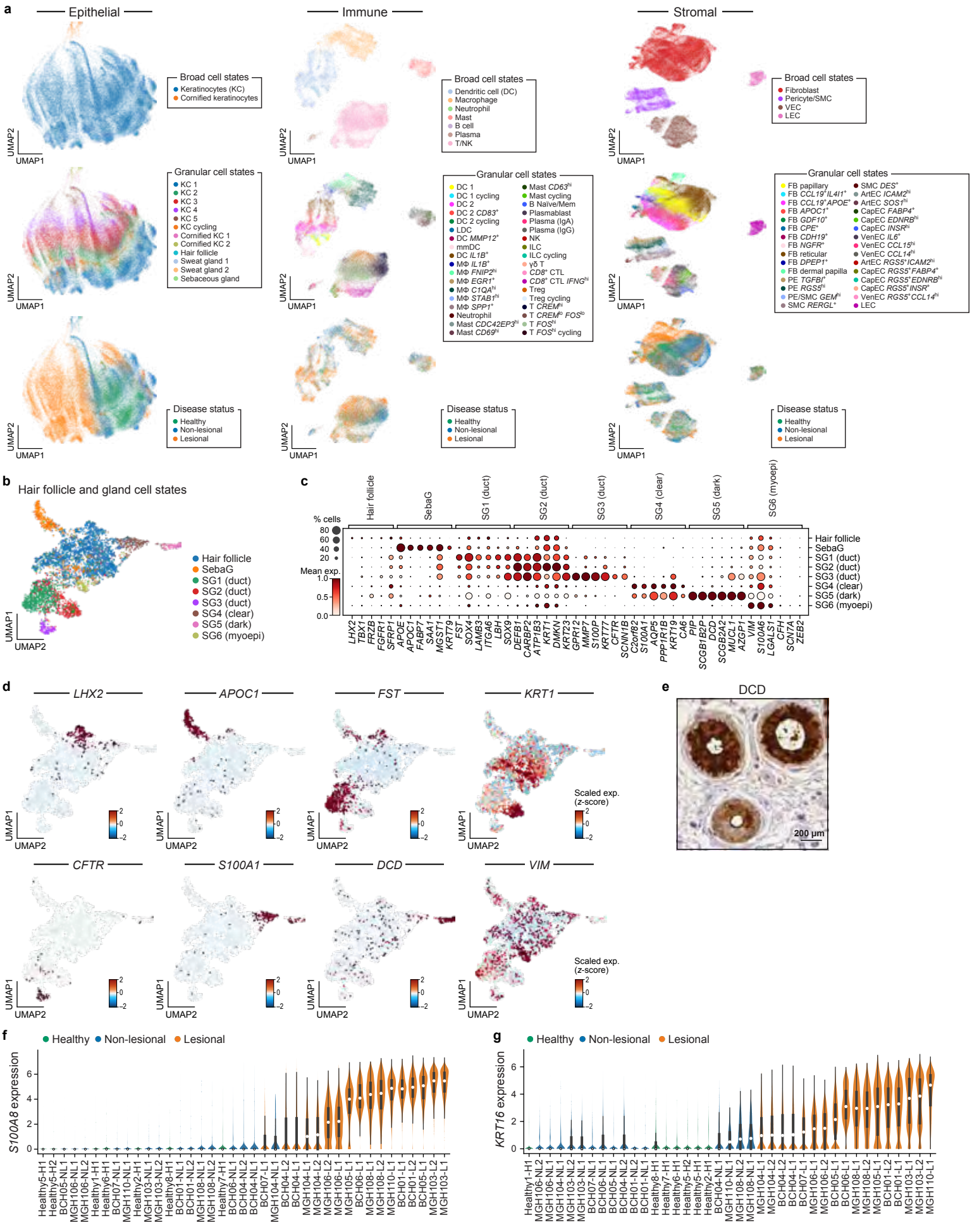
a
Epithelial
Immune
Stromal
UMAP1
UMAP2
Broad cell states
Keratinocytes (KC)
Cornified keratinocytes
Dendritic cell (DC)
Macrophage
Neutrophil
Mast
B cell
Plasma
T/NK
Fibroblast
Pericyte/SMC
VEC
LEC
Granular cell states
KC 1
KC 2
KC 3
KC 4
KC 5
KC cycling
Cornified KC 1
Cornified KC 2
Hair follicle
Sweat gland 1
Sweat gland 2
Sebaceous gland
DC 1
DC 1 cycling
DC 2
DC 2 CD83+
DC 2 cycling
LDC
DC MMP12+
mmDC
DC IL1B+
MΦ IL1B+
MΦ FNIP2hi
MΦ EGR1+
MΦ C1QAhi
MΦ STAB1hi
MΦ SPP1+
Neutrophil
Mast CDC42EP3hi
Mast CD69hi
Mast CD63hi
Mast cycling
B Naïve/Mem
Plasmablast
Plasma (IgA)
Plasma (IgG)
NK
ILC
ILC cycling
γδ T
CD8+ CTL
CD8+ CTL IFNGhi
Treg
Treg cycling
T CREMhi
T CREMlo FOSlo
T FOShi
T FOShi cycling
FB papillary
FB CCL19hiIL4I1+
FB CCL19+APOE+
FB APOC1+
FB GDF10+
FB CPE+
FB CDH19+
FB NGFR+
FB reticular
FB DPEP1+
FB dermal papilla
PE TGFBI+
PE RGS5hi
PE/SMC GEMhi
SMC RERGL+
SMC DES+
ArtEC ICAM2hi
ArtEC SOS1hi
CapEC FABP4+
CapEC EDNRBhi
CapEC INSRhi
VenEC IL6+
VenEC CCL15hi
VenEC CCL14hi
ArtEC RGS5+ICAM2hi
CapEC RGS5+FABP4+
CapEC RGS5+EDNRBhi
CapEC RGS5+INSR+
VenEC RGS5+CCL14hi
LEC
Disease status
Healthy
Non-lesional
Lesional
b
Hair follicle and gland cell states
Hair follicle
SebaG
SG1 (duct)
SG2 (duct)
SG3 (duct)
SG4 (clear)
SG5 (dark)
SG6 (myoepi)
c
% cells
Mean exp.
LHX2
TBX1
FRZB
FGFR1
SFRP1
APOE
APOC1
FABP7
SAA1
MGST1
KRT79
FST
SOX4
LAMB3
ITGA6
LBH
SOX9
DEFB1
CARBP2
ATP1B3
KRT1
DMKN
KRT23
GPR12
MMP7
S100P
KRT77
CFTR
SCNN1B
C2orf82
S100A1
AQP5
PPP1R1B
KRT19
CA6
PIP
SCGB1B2P
DCD
SCGB2A2
MUCL1
AZGP1
VIM
S100A6
LGALS1
CFH
SCN7A
ZEB2
d
LHX2
APOC1
FST
KRT1
CFTR
S100A1
DCD
VIM
Scaled exp. (z-score)
e
DCD
200 μm
f
Healthy
Non-lesional
Lesional
S100A8 expression
g
KRT16 expression

Supplementary Figure 3. Coarse and fine cell subsets in skin and skin appendages.

a, Coarse and fine cell subsets in skin. 2D embedding of epithelial (left), immune (middle) or stromal (right) scRNA-seq profiles from the entire cohort, colored by annotated coarse (top) or granular (middle) cell subsets or disease status (bottom). **b-e**, Rare hair follicle, sweat and sebaceous gland cell subsets. **b,d**, 2D embedding of scRNA-seq profiles from the entire cohort, colored by annotated granular cell subsets (b) or by z-score expression values of cell subset marker genes (d). **c**, Mean expression (dot color) and fraction of expressing cells (dot size) of hair follicle and gland subset marker genes (columns) across cell subsets (rows). **e**, Immuno-histochemistry image of sweat gland marker Dermicidin (DCD) in a healthy skin tissue section derived from the Human Protein Atlas[107]. Scale bar: 200µm. **f,g**, All lesional samples display higher expression of inflammatory epidermal markers. Distribution of the expression of *S100A8* (f, y axis) or *KRT16* (g, y axis) across each processed 10x Chromium channel (x axis). White dots: median.

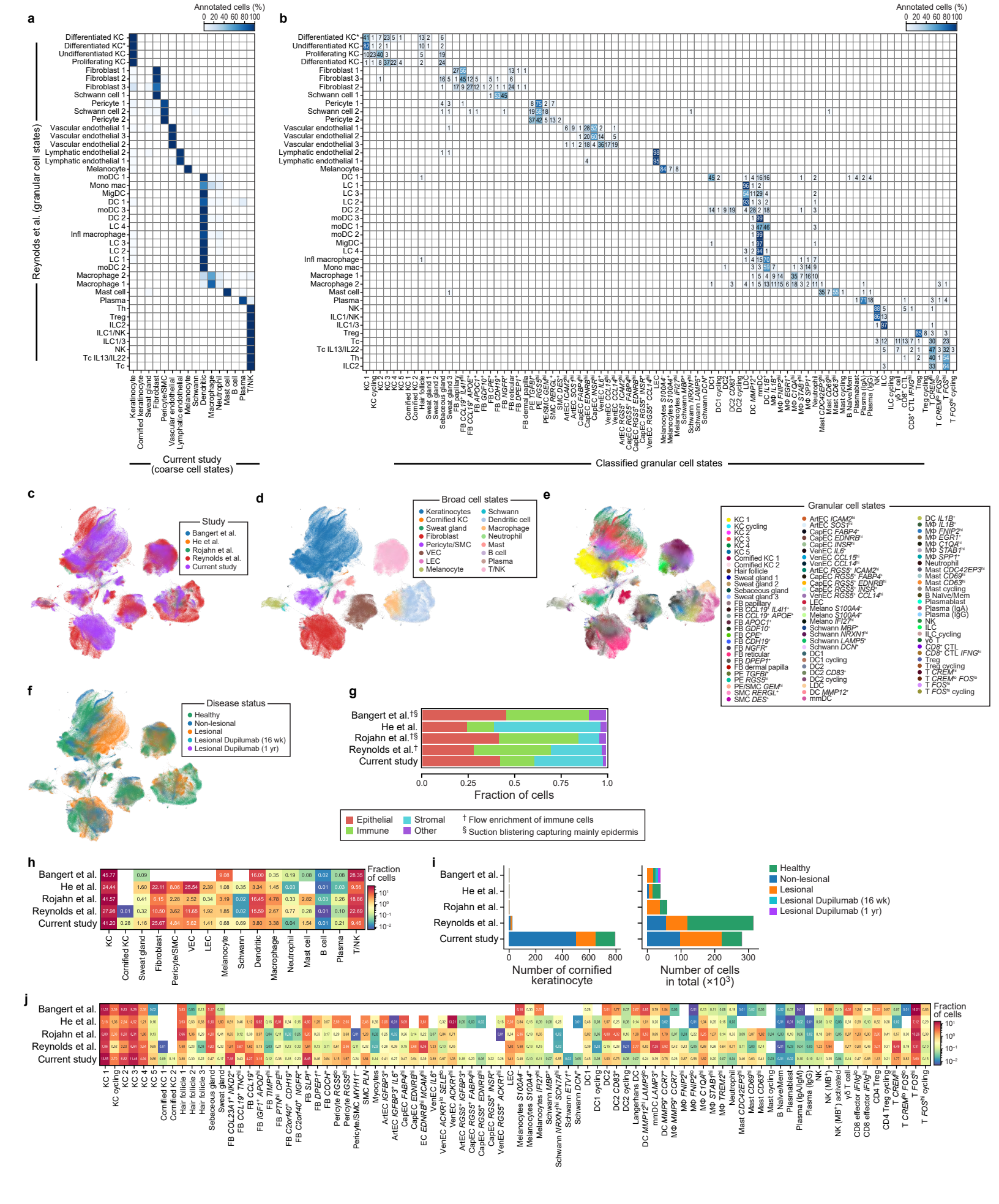
a
Annotated cells (%)
0 20 40 60 80 100
Reynolds et al. (granular cell states)
Differentiated KC
Differentiated KC*
Undifferentiated KC
Proliferating KC
Fibroblast 1
Fibroblast 2
Fibroblast 3
Schwann cell 1
Pericyte 1
Schwann cell 2
Pericyte 2
Vascular endothelial 1
Vascular endothelial 3
Vascular endothelial 2
Lymphatic endothelial 2
Lymphatic endothelial 1
Melanocyte
moDC 1
Mono mac
MigDC
DC 1
moDC 3
DC 2
LC 4
Infl macrophage
LC 3
LC 2
LC 1
moDC 2
Macrophage 2
Macrophage 1
Mast cell
Plasma
Th
Treg
ILC2
ILC1/NK
ILC1/3
NK
Tc IL13/IL22
Tc
Keratinocyte
Cornified keratinocyte
Sweat gland
Fibroblast
Pericyte/SMC
Vascular endothelial
Lymphatic endothelial
Melanocyte
Schwann
Dendritic
Macrophage
Neutrophil
Mast cell
B cell
Plasma
T/NK
Current study
(coarse cell states)
b
Annotated cells (%)
0 20 40 60 80 100
Classified granular cell states
c
Study
Bangert et al.
He et al.
Rojahn et al.
Reynolds et al.
Current study
d
Broad cell states
Keratinocytes
Cornified KC
Sweat gland
Fibroblast
Pericyte/SMC
VEC
LEC
Melanocyte
Schwann
Dendritic cell
Macrophage
Neutrophil
Mast
B cell
Plasma
T/NK
e
Granular cell states
f
Disease status
Healthy
Non-lesional
Lesional
Lesional Dupilumab (16 wk)
Lesional Dupilumab (1 yr)
g
Bangert et al.†§
He et al.
Rojahn et al.†§
Reynolds et al.†
Current study
0.0
0.25
0.5
0.75
1.0
Fraction of cells
Epithelial
Immune
Stromal
Other
† Flow enrichment of immune cells
§ Suction blistering capturing mainly epidermis
h
Bangert et al.
He et al.
Rojahn et al.
Reynolds et al.
Current study
KC
Cornified KC
Sweat gland
Fibroblast
Pericyte/SMC
VEC
LEC
Melanocyte
Schwann
Dendritic
Macrophage
Neutrophil
Mast cell
B cell
Plasma
T/NK
Fraction of cells
i
Bangert et al.
He et al.
Rojahn et al.
Reynolds et al.
Current study
0
200
400
600
800
Number of cornified keratinocyte
0
100
200
300
Number of cells in total (×10³)
Healthy
Non-lesional
Lesional
Lesional Dupilumab (16 wk)
Lesional Dupilumab (1 yr)
j
Bangert et al.
He et al.
Rojahn et al.
Reynolds et al.
Current study
Fraction of cells

Supplementary Figure 4. Integrated skin cell atlas.

a,b, Consistent cell subset annotations across datasets. Agreement (color, row-normalized) between coarse (a, columns) or granular (b, columns) cell subsets in the current study and annotations from each of four published skin scRNA-seq dataset[8,10–12] (rows) based on a linear classifier trained on the current study. **c-f**, Integrated skin atlas of current and published skin scRNA-seq datasets. 2D UMAP embedding of integrated scRNA-seq profiles (**Methods**) from the current cohort and four published datasets[8,10–12], colored by study (c), coarse cell types (d), granular cell subsets (e), or disease status (f). **g**, Cell compartment representation across studies. Proportion (x axis) of cells from each major compartment (color of bars) in each dataset (y axis). **h-j**, Cornified keratinocytes and other cell subsets absent from published data sets. **h,j**, Proportion (%) (color) of annotated coarse (h) or granular (j) subsets (columns) in the current and published studies (rows). **i**, Number (x axis) of profiled cornified keratinocytes (left) or cells overall (right) in the current and published studies (y axis). Color: condition.

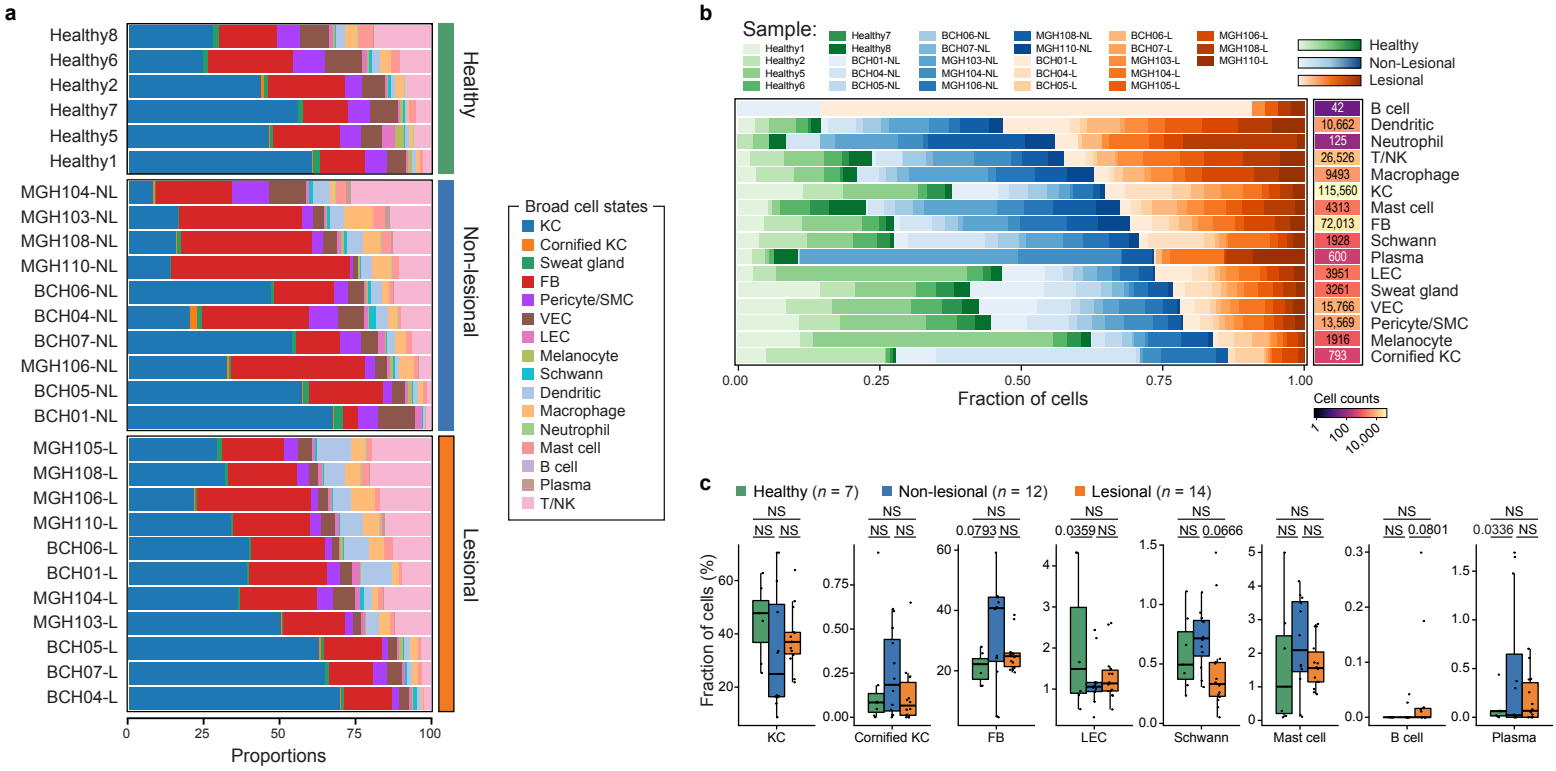
a
Healthy8
Healthy6
Healthy2
Healthy7
Healthy5
Healthy1
MGH104-NL
MGH103-NL
MGH108-NL
MGH110-NL
BCH06-NL
BCH04-NL
BCH07-NL
MGH106-NL
BCH05-NL
BCH01-NL
MGH105-L
MGH108-L
MGH106-L
MGH110-L
BCH06-L
BCH01-L
MGH104-L
MGH103-L
BCH05-L
BCH07-L
BCH04-L
Healthy
Non-lesional
Lesional
0
25
50
75
100
Proportions
Broad cell states
KC
Cornified KC
Sweat gland
FB
Pericyte/SMC
VEC
LEC
Melanocyte
Schwann
Dendritic
Macrophage
Neutrophil
Mast cell
B cell
Plasma
T/NK
b
Sample:
Healthy1
Healthy2
Healthy5
Healthy6
Healthy7
Healthy8
BCH01-NL
BCH04-NL
BCH05-NL
BCH06-NL
BCH07-NL
MGH103-NL
MGH104-NL
MGH106-NL
MGH108-NL
MGH110-NL
BCH01-L
BCH04-L
BCH05-L
BCH06-L
BCH07-L
MGH103-L
MGH104-L
MGH105-L
MGH106-L
MGH108-L
MGH110-L
Healthy
Non-Lesional
Lesional
0.00
0.25
0.50
0.75
1.00
Fraction of cells
42 B cell
10,662 Dendritic
125 Neutrophil
26,526 T/NK
9493 Macrophage
115,560 KC
4313 Mast cell
72,013 FB
1928 Schwann
600 Plasma
3951 LEC
3261 Sweat gland
15,766 VEC
13,569 Pericyte/SMC
1916 Melanocyte
793 Cornified KC
Cell counts
1
100
10,000
c
Healthy (n = 7)
Non-lesional (n = 12)
Lesional (n = 14)
Fraction of cells (%)
NS NS NS
NS NS NS
NS 0.0793 NS
NS 0.0359 NS
NS NS 0.0666
NS NS NS
NS NS 0.0801
NS 0.0336 NS
KC
Cornified KC
FB
LEC
Schwann
Mast cell
B cell
Plasma

Supplementary Figure 5. Changes in broad cell type proportions between healthy, non lesional and lesional skin.

a,b, Variation in cell proportions across individuals and conditions. **a**, Proportion (x axis) of each coarse cell types (color) in each processed sample (rows, ordered from highest to lowest immune cell proportions within each condition) in each condition (right). **b**, Proportion (x axis) of coarse cell types (rows, ordered by compartment) in healthy, non-lesional and lesional conditions in each individual (color). Left bar: total number of cells profiled of each coarse type. **c**, Differences in coarse cell types between conditions. Fraction of cells (y axis) in each condition (x axis) for each coarse category (panels). Lesional, n = 14 channels (9 samples), non-lesional, n = 12 channels (8 samples), healthy, n = 7 channels (6 samples). Center line: median; box limits: first and third quartiles; whiskers: 1.5× interquartile range. Dirichlet regression, ns: non-significant. Dots: cell type proportion by channel.

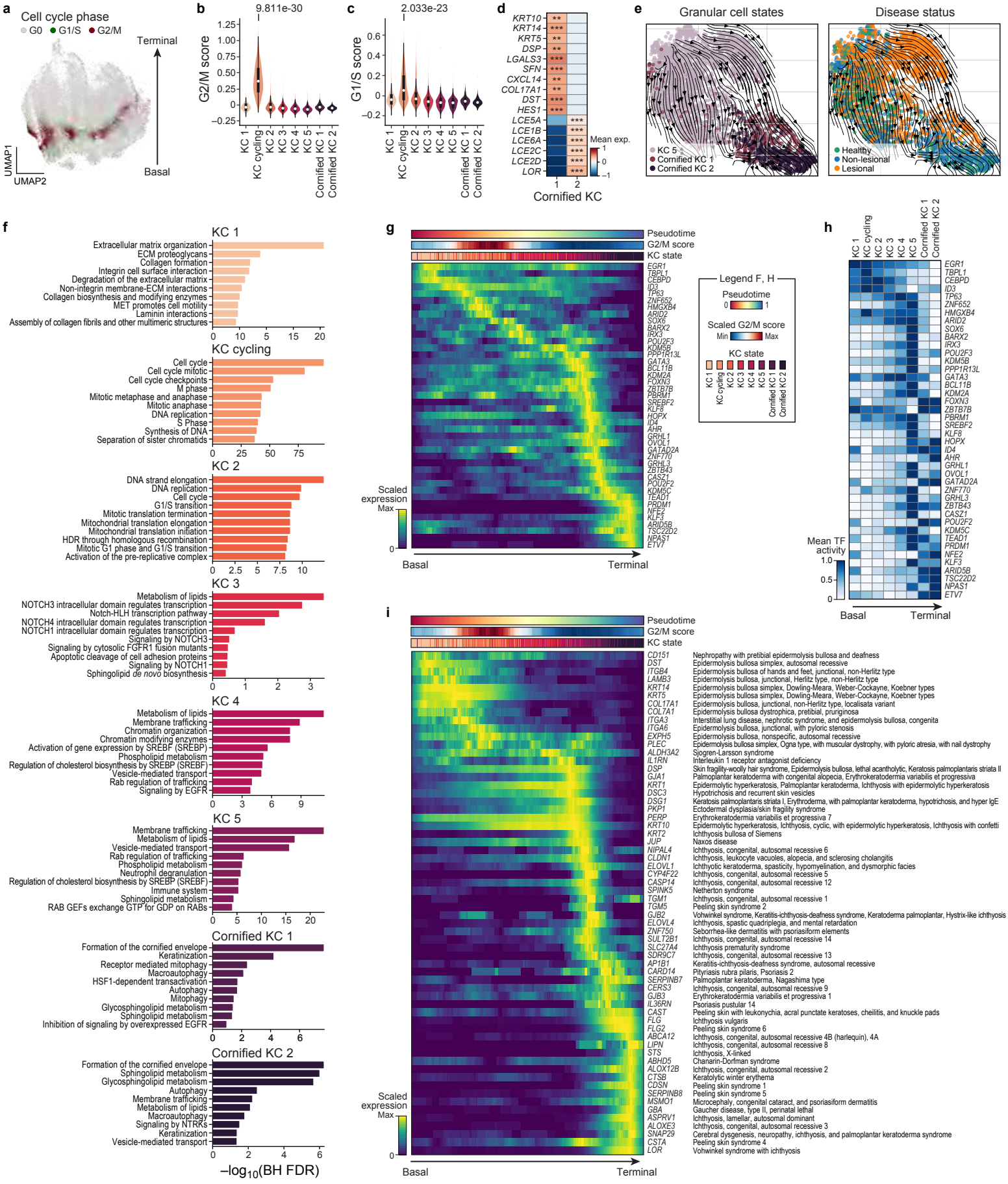
a
Cell cycle phase
G0 G1/S G2/M
Terminal
Basal
UMAP1
UMAP2
b
9.811e-30
G2/M score
c
2.033e-23
G1/S score
KC 1
KC cycling
KC 2
KC 3
KC 4
KC 5
Cornified KC 1
Cornified KC 2
d
KRT10
KRT14
KRT5
DSP
LGALS3
SFN
CXCL14
COL17A1
DST
HES1
LCE5A
LCE1B
LCE6A
LCE2C
LCE2D
LOR
Mean exp.
Cornified KC
e
Granular cell states
Disease status
Healthy
Non-lesional
Lesional
f
KC 1
Extracellular matrix organization
ECM proteoglycans
Collagen formation
Integrin cell surface interaction
Degradation of the extracellular matrix
Non-integrin membrane-ECM interactions
Collagen biosynthesis and modifying enzymes
MET promotes cell motility
Laminin interactions
Assembly of collagen fibrils and other multimeric structures
KC cycling
Cell cycle
Cell cycle mitotic
Cell cycle checkpoints
M phase
Mitotic metaphase and anaphase
Mitotic anaphase
DNA replication
S Phase
Synthesis of DNA
Separation of sister chromatids
KC 2
DNA strand elongation
DNA replication
Cell cycle
G1/S transition
Mitotic translation termination
Mitochondrial translation elongation
Mitochondrial translation initiation
HDR through homologous recombination
Mitotic G1 phase and G1/S transition
Activation of the pre-replicative complex
KC 3
Metabolism of lipids
NOTCH3 intracellular domain regulates transcription
Notch-HLH transcription pathway
NOTCH4 intracellular domain regulates transcription
NOTCH1 intracellular domain regulates transcription
Signaling by NOTCH3
Signaling by cytosolic FGFR1 fusion mutants
Apoptotic cleavage of cell adhesion proteins
Signaling by NOTCH1
Sphingolipid de novo biosynthesis
KC 4
Metabolism of lipids
Membrane trafficking
Chromatin organization
Chromatin modifying enzymes
Activation of gene expression by SREBF (SREBP)
Phospholipid metabolism
Regulation of cholesterol biosynthesis by SREBP (SREBF)
Vesicle-mediated transport
Rab regulation of trafficking
Signaling by EGFR
KC 5
Membrane trafficking
Metabolism of lipids
Vesicle-mediated transport
Rab regulation of trafficking
Phospholipid metabolism
Neutrophil degranulation
Regulation of cholesterol biosynthesis by SREBP (SREBF)
Immune system
Sphingolipid metabolism
RAB GEFs exchange GTP for GDP on RABs
Cornified KC 1
Formation of the cornified envelope
Keratinization
Receptor mediated mitophagy
Macroautophagy
HSF1-dependent transactivation
Autophagy
Mitophagy
Glycosphingolipid metabolism
Sphingolipid metabolism
Inhibition of signaling by overexpressed EGFR
Cornified KC 2
Formation of the cornified envelope
Sphingolipid metabolism
Glycosphingolipid metabolism
Autophagy
Membrane trafficking
Metabolism of lipids
Macroautophagy
Signaling by NTRKs
Keratinization
Vesicle-mediated transport
−log10(BH FDR)
g
Pseudotime
G2/M score
KC state
Scaled expression
Max
Basal
Terminal
Legend F, H
Pseudotime
Scaled G2/M score
Min
Max
KC state
h
Mean TF activity
i
CD151 Nephropathy with pretibial epidermolysis bullosa and deafness
DST Epidermolysis bullosa simplex, autosomal recessive
ITGB4 Epidermolysis bullosa of hands and feet, junctional, non-Herlitz type
LAMB3 Epidermolysis bullosa, junctional, Herlitz type, non-Herlitz type
KRT14 Epidermolysis bullosa simplex, Dowling-Meara, Weber-Cockayne, Koebner types
KRT5 Epidermolysis bullosa simplex, Dowling-Meara, Weber-Cockayne, Koebner types
COL17A1 Epidermolysis bullosa, junctional, non-Herlitz type, localisata variant
COL7A1 Epidermolysis bullosa dystrophica, pretibial, pruriginosa
ITGA3 Interstitial lung disease, nephrotic syndrome, and epidermolysis bullosa, congenita
ITGA6 Epidermolysis bullosa, junctional, with pyloric stenosis
EXPH5 Epidermolysis bullosa, nonspecific, autosomal recessive
PLEC Epidermolysis bullosa simplex, Ogna type, with muscular dystrophy, with pyloric atresia, with nail dystrophy
ALDH3A2 Sjogren-Larsson syndrome
IL1RN Interleukin 1 receptor antagonist deficiency
DSP Skin fragility-woolly hair syndrome, Epidermolysis bullosa, lethal acantholytic, Keratosis palmoplantaris striata II
GJA1 Palmoplantar keratoderma with congenital alopecia, Erythrokeratodermia variabilis et progressiva
KRT1 Epidermolytic hyperkeratosis, Palmoplantar keratoderma, Ichthyosis with epidermolytic hyperkeratosis
DSC3 Hypotrichosis and recurrent skin vesicles
DSG1 Keratosis palmoplantaris striata I, Erythroderma, with palmoplantar keratoderma, hypotrichosis, and hyper IgE
PKP1 Ectodermal dysplasia/skin fragility syndrome
PERP Erythrokeratodermia variabilis et progressiva 7
KRT10 Epidermolytic hyperkeratosis, Ichthyosis, cyclic, with epidermolytic hyperkeratosis, Ichthyosis with confetti
KRT2 Ichthyosis bullosa of Siemens
JUP Naxos disease
NIPAL4 Ichthyosis, congenital, autosomal recessive 6
CLDN1 Ichthyosis, leukocyte vacuoles, alopecia, and sclerosing cholangitis
ELOVL1 Ichthyotic keratoderma, spasticity, hypomyelination, and dysmorphic facies
CYP4F22 Ichthyosis, congenital, autosomal recessive 5
CASP14 Ichthyosis, congenital, autosomal recessive 12
SPINK5 Netherton syndrome
TGM1 Ichthyosis, congenital, autosomal recessive 1
TGM5 Peeling skin syndrome 2
GJB2 Vohwinkel syndrome, Keratitis-ichthyosis-deafness syndrome, Keratoderma palmoplantar, Hystrix-like ichthyosis
ELOVL4 Ichthyosis, spastic quadriplegia, and mental retardation
ZNF750 Seborrhea-like dermatitis with psoriasiform elements
SULT2B1 Ichthyosis, congenital, autosomal recessive 14
SLC27A4 Ichthyosis prematurity syndrome
SDR9C7 Ichthyosis, congenital, autosomal recessive 13
AP1B1 Keratitis-ichthyosis-deafness syndrome, autosomal recessive
CARD14 Pityriasis rubra pilaris, Psoriasis 2
SERPINB7 Palmoplantar keratoderma, Nagashima type
CERS3 Ichthyosis, congenital, autosomal recessive 9
GJB3 Erythrokeratodermia variabilis et progressiva 1
IL36RN Psoriasis pustular 14
CAST Peeling skin with leukonychia, acral punctate keratoses, cheilitis, and knuckle pads
FLG Ichthyosis vulgaris
FLG2 Peeling skin syndrome 6
ABCA12 Ichthyosis, congenital, autosomal recessive 4B (harlequin), 4A
LIPN Ichthyosis, congenital, autosomal recessive 8
STS Ichthyosis, X-linked
ABHD5 Chanarin-Dorfman syndrome
ALOX12B Ichthyosis, congenital, autosomal recessive 2
CTSB Keratolytic winter erythema
CDSN Peeling skin syndrome 1
SERPINB8 Peeling skin syndrome 5
MSMO1 Microcephaly, congenital cataract, and psoriasiform dermatitis
GBA Gaucher disease, type II, perinatal lethal
ASPRV1 Ichthyosis, lamellar, autosomal dominant
ALOXE3 Ichthyosis, congenital, autosomal recessive 3
SNAP29 Cerebral dysgenesis, neuropathy, ichthyosis, and palmoplantar keratoderma syndrome
CSTA Peeling skin syndrome 4
LOR Vohwinkel syndrome with ichthyosis

Supplementary Figure 6. Keratinocyte differentiation continuum in adult skin.

a-c, Identification of cycling keratinocytes. **a**, 2D embedding of keratinocyte scRNA-seq profiles colored by cell cycle phase (**Methods**). Arrow: differentiation axis from basal to terminal KCs. **b,c**, Distribution of G2/M (b) and S (c) phase scores (y axis) in KC subsets (x axis). BH FDR is shown (two-sided Welch's t test on per channel mean adjusted for multiple testing). **d**, Higher expression of late cornified envelope genes in cornified KC2s. Mean z-scored expression values (color) of genes (columns) differentially expressed between cornified KC1s and KC2s (rows). BH FDR: **<0.01, ***<0.001 (Welch's t test); exact FDR values are listed in the Source Data file. **e**, Cornification trajectories in healthy, non-lesional and lesional skin. RNA velocities (arrows) projected onto 2D UMAP embedding of scRNA-seq profiles of KC5s, cornified KC1s and cornified KC2s in healthy, non-lesional and lesional skin colored by cell subset (left) or disease status (right). **f**, Enriched pathways and processes in different KC subsets recapitulate human skin biology. Reactome[109] terms (rows) that are significantly enriched (x axis, $-\log_{10}$(BH FDR), Fisher's exact test, **Methods**) in each KC subset. **g-i**, TF and monogenic skin disease temporal gene expression along KC differentiation follows function and phenotype. **g,i**, Scaled expression values (color) of TF encoding genes (g, rows) or monogenic skin disease genes from OMIM (i, rows) in cells (g,i, columns) from healthy controls skin ordered along DPT representing keratinocyte differentiation from basal (left) to terminal cornified (right) cells. Colored bars: DPT (top), G2/M score (middle) and annotated KC subset (bottom). Data were downsampled (**Methods**) and equal numbers of cells for each KC subset are shown. **h**, Predicted mean TF activity (color) (**Methods**) for each TF gene in (g) across KC subsets (columns) from basal (left) to terminal (right).

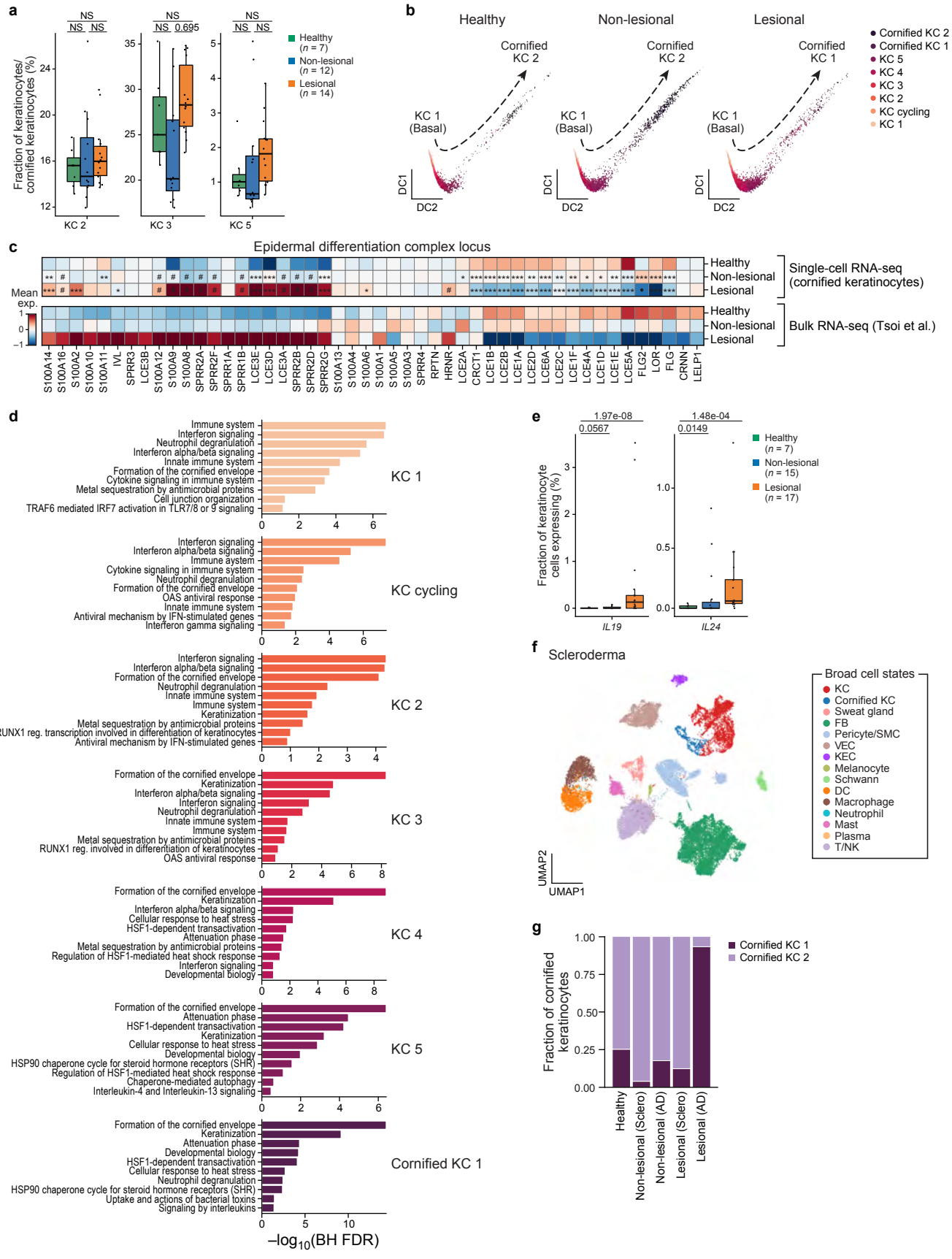
a
NS
NS NS
NS
NS 0.695
NS
NS NS
Fraction of keratinocytes/ cornified keratinocytes (%)
KC 2
KC 3
KC 5
Healthy (n = 7)
Non-lesional (n = 12)
Lesional (n = 14)
b
Healthy
Non-lesional
Lesional
Cornified KC 2
Cornified KC 1
KC 1 (Basal)
DC1
DC2
Cornified KC 2
KC 5
KC 4
KC 3
KC 2
KC cycling
KC 1
c
Epidermal differentiation complex locus
Mean exp.
Healthy
Non-lesional
Lesional
Single-cell RNA-seq (cornified keratinocytes)
Bulk RNA-seq (Tsoi et al.)
S100A14 S100A16 S100A2 S100A10 S100A11 IVL SPRR3 LCE3B S100A12 S100A9 S100A8 SPRR2A SPRR2F SPRR1A SPRR1B LCE3E LCE3D LCE3A SPRR2B SPRR2D SPRR2G S100A13 S100A4 S100A6 S100A1 S100A5 S100A3 SPRR4 RPTN HRNR LCE2A CRCT1 LCE1B LCE2B LCE1A LCE2D LCE6A LCE2C LCE1F LCE4A LCE1D LCE1E LCE5A FLG2 LOR FLG CRNN LELP1
d
Immune system
Interferon signaling
Neutrophil degranulation
Interferon alpha/beta signaling
Innate immune system
Formation of the cornified envelope
Cytokine signaling in immune system
Metal sequestration by antimicrobial proteins
Cell junction organization
TRAF6 mediated IRF7 activation in TLR7/8 or 9 signaling
KC 1
Interferon signaling
Interferon alpha/beta signaling
Immune system
Cytokine signaling in immune system
Neutrophil degranulation
Formation of the cornified envelope
OAS antiviral response
Innate immune system
Antiviral mechanism by IFN-stimulated genes
Interferon gamma signaling
KC cycling
Interferon signaling
Interferon alpha/beta signaling
Formation of the cornified envelope
Neutrophil degranulation
Innate immune system
Immune system
Keratinization
Metal sequestration by antimicrobial proteins
RUNX1 reg. transcription involved in differentiation of keratinocytes
Antiviral mechanism by IFN-stimulated genes
KC 2
Formation of the cornified envelope
Keratinization
Interferon alpha/beta signaling
Interferon signaling
Neutrophil degranulation
Innate immune system
Immune system
Metal sequestration by antimicrobial proteins
RUNX1 reg. involved in differentiation of keratinocytes
OAS antiviral response
KC 3
Formation of the cornified envelope
Keratinization
Interferon alpha/beta signaling
Cellular response to heat stress
HSF1-dependent transactivation
Attenuation phase
Metal sequestration by antimicrobial proteins
Regulation of HSF1-mediated heat shock response
Interferon signaling
Developmental biology
KC 4
Formation of the cornified envelope
Attenuation phase
HSF1-dependent transactivation
Keratinization
Cellular response to heat stress
Developmental biology
HSP90 chaperone cycle for steroid hormone receptors (SHR)
Regulation of HSF1-mediated heat shock response
Chaperone-mediated autophagy
Interleukin-4 and Interleukin-13 signaling
KC 5
Formation of the cornified envelope
Keratinization
Attenuation phase
Developmental biology
HSF1-dependent transactivation
Cellular response to heat stress
Neutrophil degranulation
HSP90 chaperone cycle for steroid hormone receptors (SHR)
Uptake and actions of bacterial toxins
Signaling by interleukins
Cornified KC 1
–log10(BH FDR)
e
1.97e-08
0.0567
1.48e-04
0.0149
Fraction of keratinocyte cells expressing (%)
IL19
IL24
Healthy (n = 7)
Non-lesional (n = 15)
Lesional (n = 17)
f
Scleroderma
UMAP2
UMAP1
Broad cell states
KC
Cornified KC
Sweat gland
FB
Pericyte/SMC
VEC
KEC
Melanocyte
Schwann
DC
Macrophage
Neutrophil
Mast
Plasma
T/NK
g
Fraction of cornified keratinocytes
Cornified KC 1
Cornified KC 2
Healthy
Non-lesional (Sclero)
Non-lesional (AD)
Lesional (Sclero)
Lesional (AD)

Supplementary Figure 7. Remodeling of KC expression and cornification in lesional AD skin.

a, Changes in KC subset composition. Proportions (y axis) of KC subsets (x axis) in each disease condition (colored bars). Lesional, n = 14 channels (9 samples), non-lesional, n = 12 channels (8 samples), healthy, n = 7 channels (6 samples). Center line: median; box limits: first and third quartiles; whiskers: 1.5× interquartile range; Dots: cell type proportion by channel. **b**, Near absence of KC2s in lesional AD skin. 2D diffusion map of KC scRNA- seq profiles from healthy (left), non-lesional (middle) and lesional (right) skin colored by KC subset. Arrows: differentiation trajectory from basal to terminal cornified KCs. **c**, Expression changes in cornified KCs and in bulk RNA-seq. Mean z-scored expression values (color) of genes (columns) differentially expressed (by scRNA-seq) in cornified keratinocytes between conditions (rows) in scRNA-seq profiles (top) and in bulk RNA-seq[19] (bottom). BH FDR: #<0.1, *<0.05, **<0.01, ***<0.001; exact FDR values are provided in the Source Data file. **d**, Enriched pathways and processes in KC subsets in AD lesional skin. Top 10 most significant Reactome[109] terms (rows) (x axis, -$\log_{10}$(BH FDR), Fisher's exact test, DEGs with FDR < 0.1, |log2FC|>0.5 were used) in each KC subset (colors) (**STAR Methods**). **e**, Fraction of keratinocytes (y axis) expressing *IL19* (left) and *IL24* (right) in healthy, non-lesional and lesional conditions (x-axis). Lesional, n = 17 channels (11 samples), non-lesional, n = 15 channels (10 samples), healthy, n = 7 channels (6 samples). Center line: median; box limits: first and third quartiles; whiskers: 1.5× interquartile range. pvalues, (Mann-Whitney U test). Dots*:* cell type proportion by channel. **f,g**, Decreased abundance of cornified KC2s and increased abundance of cycling KC2s are features of lesional atopic dermatitis skin but not observed in scleroderma scRNA-seq. **f**, 2D embedding of scRNA-seq profiles from 7 healthy donors and two scleroderma patients, colored by annotated coarse cell types. **g**, Proportion of cornified KC1s and KC2s (y axis) in healthy, scleroderma and AD skin (columns).

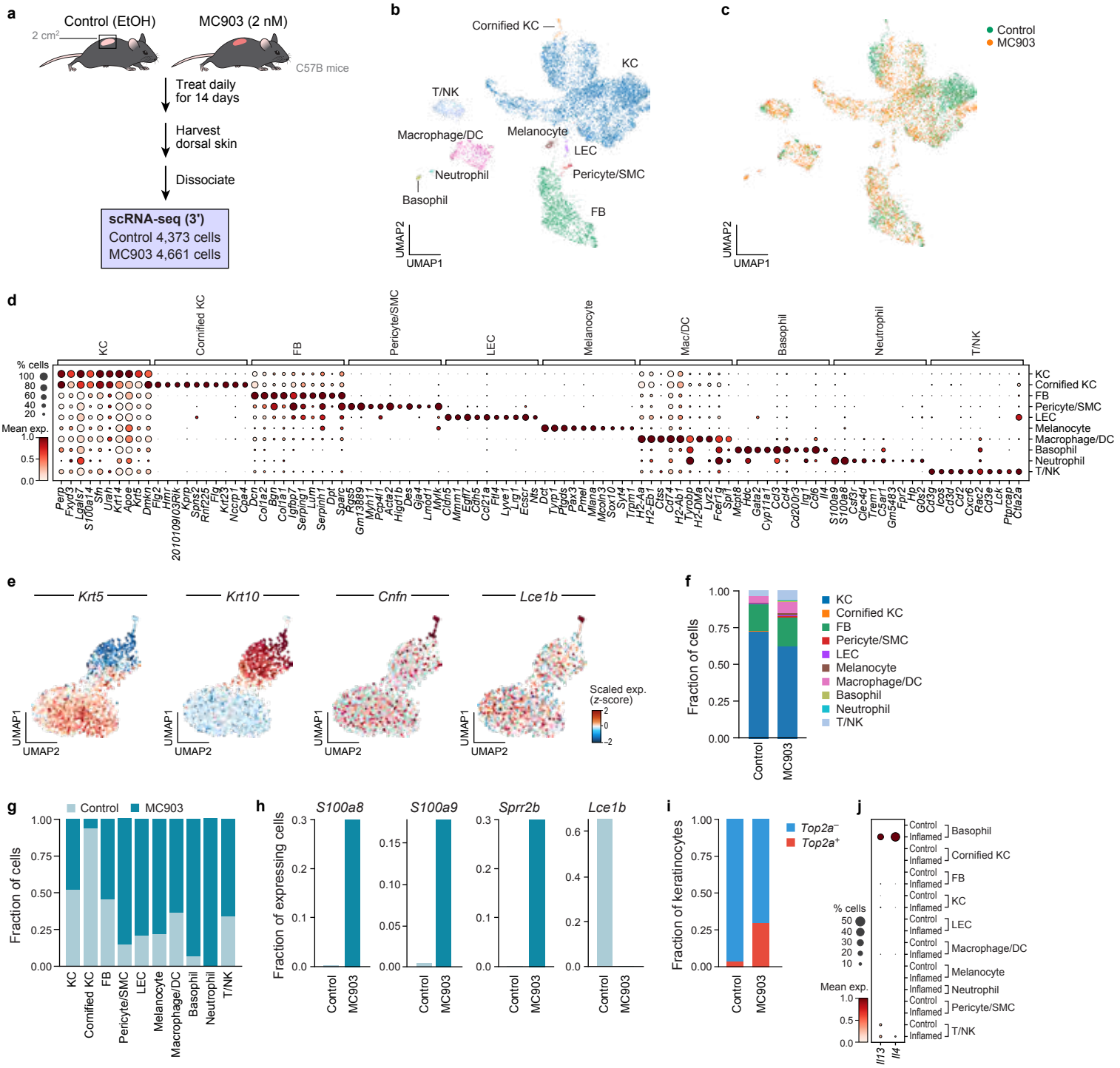
a
Control (EtOH)
MC903 (2 nM)
2 cm²
C57B mice
Treat daily for 14 days
Harvest dorsal skin
Dissociate
scRNA-seq (3')
Control 4,373 cells
MC903 4,661 cells
b
Cornified KC
KC
T/NK
Macrophage/DC
Melanocyte
LEC
Neutrophil
Pericyte/SMC
Basophil
FB
UMAP2
UMAP1
c
Control
MC903
UMAP2
UMAP1
d
KC
Cornified KC
FB
Pericyte/SMC
LEC
Melanocyte
Mac/DC
Basophil
Neutrophil
T/NK
% cells
Mean exp.
e
Krt5
Krt10
Cnfn
Lce1b
Scaled exp. (z-score)
UMAP1
UMAP2
f
Fraction of cells
KC
Cornified KC
FB
Pericyte/SMC
LEC
Melanocyte
Macrophage/DC
Basophil
Neutrophil
T/NK
Control
MC903
g
Control
MC903
Fraction of cells
h
S100a8
S100a9
Sprr2b
Lce1b
Fraction of expressing cells
i
Top2a⁻
Top2a⁺
Fraction of keratinocytes
j
% cells
Mean exp.
Control
Inflamed
Basophil
Cornified KC
FB
KC
LEC
Macrophage/DC
Melanocyte
Neutrophil
Pericyte/SMC
T/NK
Il13
Il4

Supplementary Figure 8. The MC903 mouse model of skin inflammation recapitulates aspects of human atopic dermatitis within the KC compartment.

a-c, Mouse skin scRNA-seq in uninflamed and MC903-induced inflammation. **a**, Experiment overview (**Methods**). **b,c**, 2D embedding of scRNA-seq profiles from control and MC903-treated mice, colored by annotated coarse cell types (b) or by treatment (c). **d**, Mean expression (dot color) and proportion of expressing cells (dot size) of coarse cell type marker genes (columns) in each coarse cell type (rows). **e**, Conserved KC differentiation trajectory across species. 2D embedding of KC scRNA-seq profiles from control mice, colored by z-scored expression values of human KC subset markers. **f-i**, MC903-induced inflammation mimics multiple cell composition and expression changes of human AD skin. **f**, Proportion (y axis) of cells of each coarse type (color) across conditions (columns). **g**, Infiltration of neutrophils and basophils and near absence of cornified KCs and in MC903-treated skin. Proportion of cells (y axis) from untreated and treated mice (color) in each coarse cell type (x axis). **h,i**, Increased expression of epidermal inflammation markers and KC cycling, and decrease of late cornified envelope transcripts. Proportion (y axis) of KCs expressing specific marker genes in control and MC903-treated mice (color). **j**, Mean expression (dot color; min-max scaled log(TP10K+1)) and fraction of expressing cells (dot size) of *Il13* and *Il4* (columns) in broad cell types in control and MC903-treated skin (rows).

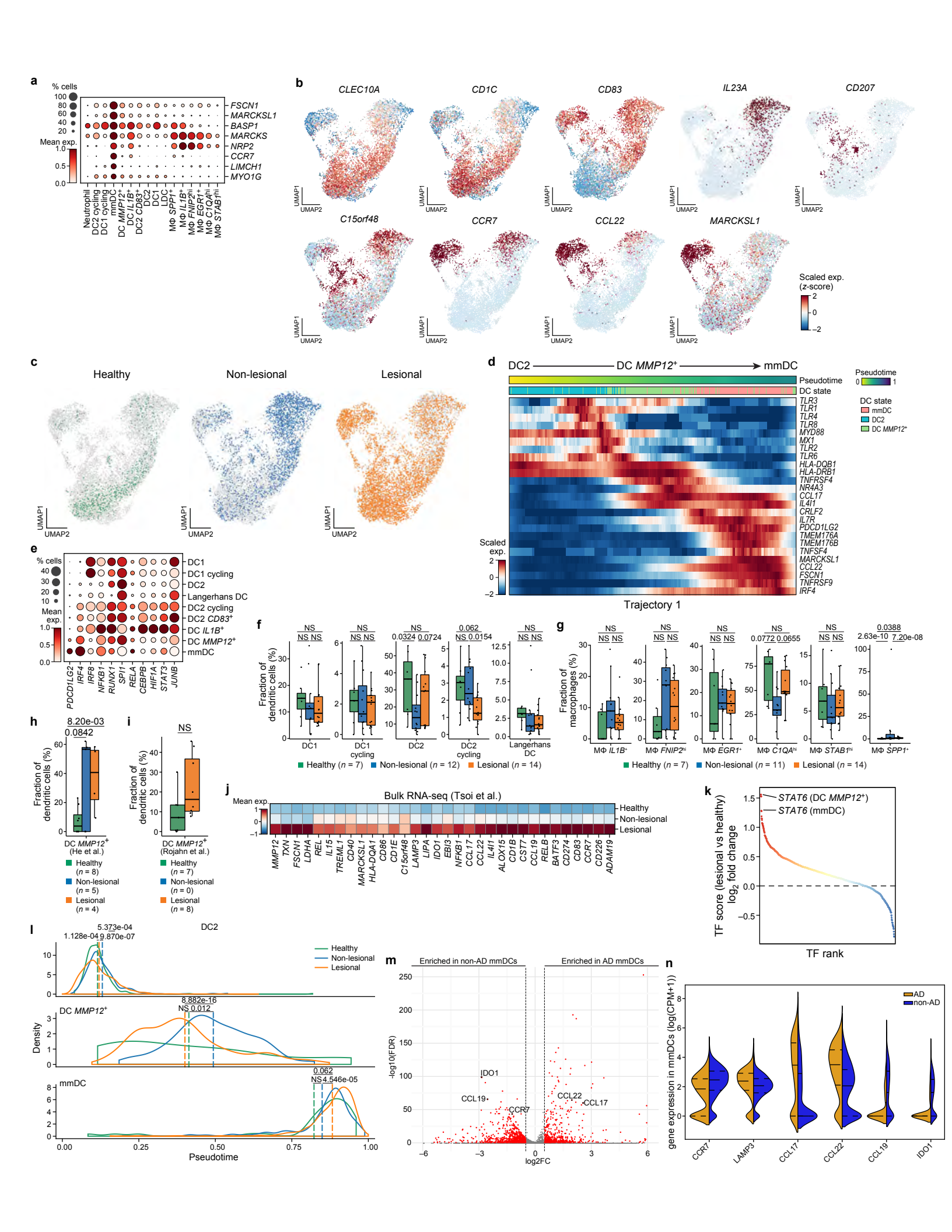
a
% cells
Mean exp.
FSCN1
MARCKSL1
BASP1
MARCKS
NRP2
CCR7
LIMCH1
MYO1G
Neutrophil
DC2 cycling
DC1 cycling
mmDC
DC MMP12+
DC IL1B+
DC2 CD83+
DC2
DC1
LDC
MΦ SPP1+
MΦ IL1B+
MΦ FNIP2hi
MΦ EGR1+
MΦ C1QAhi
MΦ STAB1hi
b
CLEC10A
CD1C
CD83
IL23A
CD207
C15orf48
CCR7
CCL22
MARCKSL1
UMAP1
UMAP2
Scaled exp. (z-score)
c
Healthy
Non-lesional
Lesional
d
DC2
DC MMP12+
mmDC
Pseudotime
DC state
Scaled exp.
TLR3
TLR1
TLR4
TLR8
MYD88
MX1
TLR2
TLR6
HLA-DQB1
HLA-DRB1
TNFRSF4
NR4A3
CCL17
IL4I1
CRLF2
IL7R
PDCD1LG2
TMEM176A
TMEM176B
TNFSF4
MARCKSL1
CCL22
FSCN1
TNFRSF9
IRF4
Trajectory 1
e
% cells
Mean exp.
DC1
DC1 cycling
DC2
Langerhans DC
DC2 cycling
DC2 CD83+
DC IL1B+
DC MMP12+
mmDC
PDCD1LG2
IRF4
IRF8
NFKB1
RUNX1
SPI1
RELA
CEBPB
HIF1A
STAT3
JUNB
f
Fraction of dendritic cells (%)
DC1
DC1 cycling
DC2
DC2 cycling
Langerhans DC
Healthy (n = 7)
Non-lesional (n = 12)
Lesional (n = 14)
g
Fraction of macrophages (%)
MΦ IL1B+
MΦ FNIP2hi
MΦ EGR1+
MΦ C1QAhi
MΦ STAB1hi
MΦ SPP1+
Healthy (n = 7)
Non-lesional (n = 11)
Lesional (n = 14)
h
8.20e-03
0.0842
Fraction of dendritic cells (%)
DC MMP12+ (He et al.)
Healthy (n = 8)
Non-lesional (n = 5)
Lesional (n = 4)
i
NS
Fraction of dendritic cells (%)
DC MMP12+ (Rojahn et al.)
Healthy (n = 7)
Non-lesional (n = 0)
Lesional (n = 8)
j
Bulk RNA-seq (Tsoi et al.)
Mean exp.
Healthy
Non-lesional
Lesional
MMP12
TXN
FSCN1
LDHA
REL
IL15
TREML1
CD40
MARCKSL1
HLA-DQA1
CD86
CD1E
C15orf48
LAMP3
LIPA
IDO1
EBI3
NFKB1
CCL17
CCL22
IL4I1
ALOX15
CD1B
CST7
CCL19
RELB
BATF3
CD274
CD83
CCR7
CD226
ADAM19
k
STAT6 (DC MMP12+)
STAT6 (mmDC)
TF score (lesional vs healthy) log2 fold change
TF rank
l
DC2
DC MMP12+
mmDC
Healthy
Non-lesional
Lesional
Density
Pseudotime
m
Enriched in non-AD mmDCs
Enriched in AD mmDCs
-log10(FDR)
log2FC
IDO1
CCL19
CCR7
CCL22
CCL17
n
AD
non-AD
gene expression in mmDCs (log(CPM+1))
CCR7
LAMP3
CCL17
CCL22
CCL19
IDO1

Supplementary Figure 9. A shift in DC activation trajectories towards a mature migratory state in lesional AD skin.

a-c, mmDCs express a migratory expression signature. **a**, Mean expression (dot color) and fraction of expressing cells (dot size) of actin cytoskeleton or cell migration genes (rows) in myeloid cell subsets (columns). **b,c**, 2D embedding of DC scRNA-seq profiles from healthy and AD skin, colored by expression of marker genes (b, z score) or by disease condition (c). **d**, DC activation trajectory. Expression of DC subset marker genes (rows) in cells (columns) from healthy, non-lesional or lesional skin ordered by DPT (top color bar) along DC activation trajectory and labeled by subset (bottom color bar, as in **Fig. 3d**). Data were downsampled (**Methods**) and equal numbers of cells for each cell subset are shown. **e**, Key TF regulators of DCs. Mean expression (dot color) and fraction of expressing cells (dot size) of key DC TF genes (columns) in each DC subset (rows). **f,g**, Changes in myeloid cell composition across conditions. Proportion of cells (y axis) in different DC (f) and macrophage (g) subsets in each condition (x axis). Lesional, n = 14 channels (9 samples), non-lesional, n = 12 channels (8 samples), healthy, n = 7 channels (6 samples). Center line: median; box limits: first and third quartiles; whiskers: 1.5× interquartile range. ns: non-significant; Dirichlet regression, ns: non-significant. Dots: cell type proportion by channel. **h-j**, Increased DC *MMP12*$^{+}$ cells in AD. **h,i**, Proportion of *MMP12*$^{+}$ DC within DCs (y axis) in each condition (x axis) in published scRNA-Seq (h[8], and i[11]). Dots: cell type proportion by sample. **j**, Mean expression (color, z-score) of mmDC and *MMP12*$^{+}$ DC marker genes (columns) across conditions (rows) in bulk RNA-Seq[19]. **k**, High inferred STAT6 activity in *MMP12*$^{+}$ DCs and mmDCs. Differentially TF activity scores (y axis; lesional - healthy) for each TF in each myeloid cell subset (dot) sorted by TF rank (x axis) (**Methods**). **l**, Aberrant DC differentiation trajectories in AD skin. Distribution of diffusion pseudotimes (DPT, x axis, **Methods**) for DC2s (top),

MMP12^{+} DCs (middle) and mmDCs (bottom) in each condition (color). BH FDR, Mann-Whitney U test. Vertical dashed lines: median. **m**, Differentially expressed genes in mmDCs from lesional AD skin. Effect size (x axis, $\log_2$(fold change)) and significance (y axis, -$\log_{10}$(FDR), wilcoxon t test) of differential gene expression between mmDCs from lesional AD *vs*. nonlesional cells. Red: significant genes (FDR<0.1 and abs(log fold-change)>0.5). **n**, Gene expression of mmDC marker genes in mmDCs from AD (brown) or non-AD (blue) cells. Boxplots for **f-i**: center line, median; box limits, first and third quartiles; whiskers, 1.5× interquartile range.

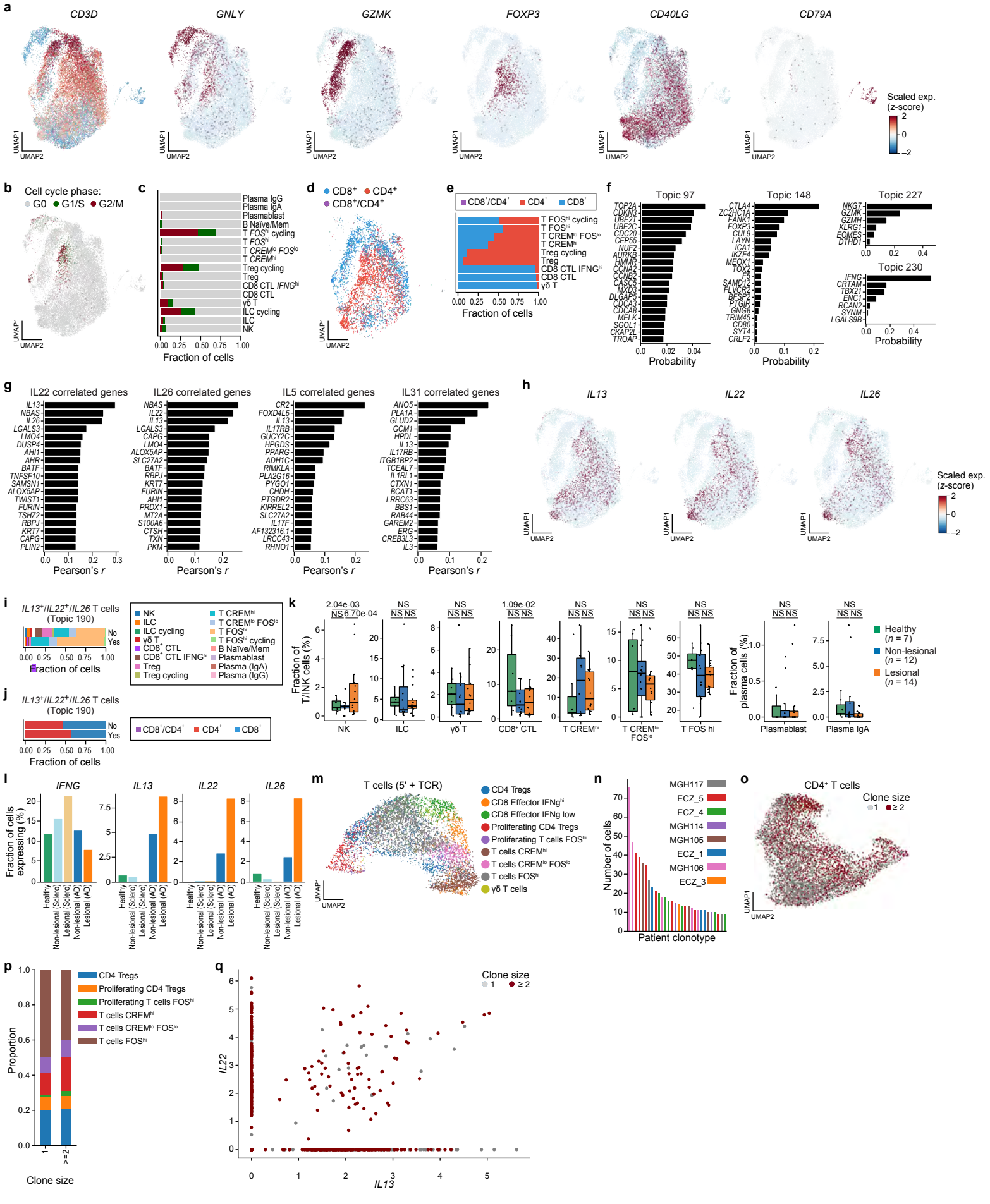
a
CD3D
GNLY
GZMK
FOXP3
CD40LG
CD79A
UMAP1
UMAP2
Scaled exp. (z-score)
b
Cell cycle phase:
G0
G1/S
G2/M
c
Plasma IgG
Plasma IgA
Plasmablast
B Naive/Mem
T FOS^hi cycling
T FOS^hi
T CREM^lo FOS^lo
T CREM^hi
Treg cycling
Treg
CD8 CTL IFNG^hi
CD8 CTL
γδ T
ILC cycling
ILC
NK
Fraction of cells
d
CD8+
CD4+
CD8+/CD4+
e
CD8+/CD4+
CD4+
CD8+
T FOS^hi cycling
T FOS^hi
T CREM^lo FOS^lo
T CREM^hi
Treg cycling
Treg
CD8 CTL IFNG^hi
CD8 CTL
γδ T
Fraction of cells
f
Topic 97
Topic 148
Topic 227
Topic 230
Probability
g
IL22 correlated genes
IL26 correlated genes
IL5 correlated genes
IL31 correlated genes
Pearson's r
h
IL13
IL22
IL26
Scaled exp. (z-score)
i
IL13+/IL22+/IL26 T cells (Topic 190)
No
Yes
Fraction of cells
NK
ILC
ILC cycling
γδ T
CD8+ CTL
CD8+ CTL IFNG^hi
Treg
Treg cycling
T CREM^hi
T CREM^lo FOS^lo
T FOS^hi
T FOS^hi cycling
B Naïve/Mem
Plasmablast
Plasma (IgA)
Plasma (IgG)
j
IL13+/IL22+/IL26 T cells (Topic 190)
No
Yes
Fraction of cells
CD8+/CD4+
CD4+
CD8+
k
2.04e-03
NS
6.70e-04
NS
NS
NS
NS
1.09e-02
NS
NS
NS
NS
NS
NS
NS
NS
NS
NS
NS
NS
Fraction of T/INK cells (%)
NK
ILC
γδ T
CD8+ CTL
T CREM^hi
T CREM^lo FOS^lo
T FOS hi
Fraction of plasma cells (%)
Plasmablast
Plasma IgA
Healthy (n = 7)
Non-lesional (n = 12)
Lesional (n = 14)
l
IFNG
IL13
IL22
IL26
Fraction of cells expressing (%)
Healthy
Non-lesional (Sclero)
Lesional (Sclero)
Non-lesional (AD)
Lesional (AD)
m
T cells (5' + TCR)
CD4 Tregs
CD8 Effector IFNg^hi
CD8 Effector IFNg low
Proliferating CD4 Tregs
Proliferating T cells FOS^hi
T cells CREM^hi
T cells CREM^lo FOS^lo
T cells FOS^hi
γδ T cells
n
Number of cells
Patient clonotype
MGH117
ECZ_5
ECZ_4
MGH114
MGH105
ECZ_1
MGH106
ECZ_3
o
CD4+ T cells
Clone size
1
≥ 2
p
Proportion
CD4 Tregs
Proliferating CD4 Tregs
Proliferating T cells FOS^hi
T cells CREM^hi
T cells CREM^lo FOS^lo
T cells FOS^hi
Clone size
q
Clone size
1
≥ 2
IL22
IL13

Supplementary Figure 10. Characterization of skin lymphocytes and expanded effector *IL13/IL22/IL26* co-expressing T cells.

a-e, Lymphocyte subsets in healthy and inflamed human skin tissue. **a-d**, 2D embedding of scRNA-seq profiles of lymphocytes from healthy and AD skin, colored by expression of indicated marker genes (a, z score), cell cycle phase (b) or *CD4*/*CD8* status (d). **c**, Cycling lymphocyte subsets. Proportion (x axis) of lymphocytes in each cell cycle phase (color, as in **b**) from each subset (rows). **e**, CD4/CD8 T cell subsets. Proportion (x axis) of $CD4^+$ or $CD8^+$ cells (color, as in D) in each T cell subset (rows). **f**, Lymphocyte gene programs. Probabilities (x axis) of top scoring genes (y axis) in each topic. **g-h**, Co-expression of *IL13, IL22* and *IL26* across lymphocytes in lesional skin. **g**, Pearson's correlation coefficient (r, x axis) for the top genes (y axis) correlated with *IL22, IL26, IL5* or *IL31* across lymphocytes, rank ordered by correlation. **h**, 2D embedding of lymphocyte scRNA-seq profiles from healthy and AD skin, colored expression of *IL13, IL22* or *IL26* (z score). **i,j**, Distribution of $IL13^+/IL22^+/IL26^+$ co-expressing T cells across lymphocyte subsets. Proportion (x axis) of $IL13^+/IL22^+/IL26^+$ co-expressing T cells ("yes") and all other T cells ("no") from each lymphocyte subset (i, color) or from $CD4^+$, $CD8^+$, and $CD4^+/CD8^+$ cells (j, color). **k**, Lymphocyte subsets (T cells/ILCs/plasma cells) that do not change in proportion between conditions. Proportions (y axis) of lymphocyte subsets (x axis) in each condition (*x* axis, color). Lesional, n = 14 channels (9 samples), non-lesional, n = 12 channels (8 samples), healthy, n = 7 channels (6 samples). Center line: median; box limits: first and third quartiles; whiskers: 1.5× interquartile range. Dirichlet regression, ns: non-significant. Dots: cell type proportion by channel. **l**, $IL13^+/IL22^+/IL26^+$ expressing T cells are detected in lesional AD but not scleroderma skin. Fraction of lymphocytes (y axis) expressing *IFNG*, *IL13*, *IL22*, or *IL26* in each condition (*x* axis, color). **m-p**, T cell clonality analysis. **m**, UMAP embedding of 5' scRNA-seq profiles (dots)

of T cells from lesional AD skin, colored by cell type (*n*=7,256 cells). **n**, T cell clone size (y-axis) for largest clones (x axis) detected across eight patients (color). **o**, UMAP embedding of 5' scRNA-seq profiles of CD4+ T cells colored by clone size (*n*=6,047 cells). **p**, Proportion (x axis) of CD4 + T cell subsets in expanded (≥2) or non-expanded (1) T cells. **q**, Expanded *IL22/IL13* co-expressing CD4+ T cells. *IL22* (y axis) and *IL13* (x axis) gene expression in CD4+ T cells from expanded (red) and non-expanded (grey) clones.

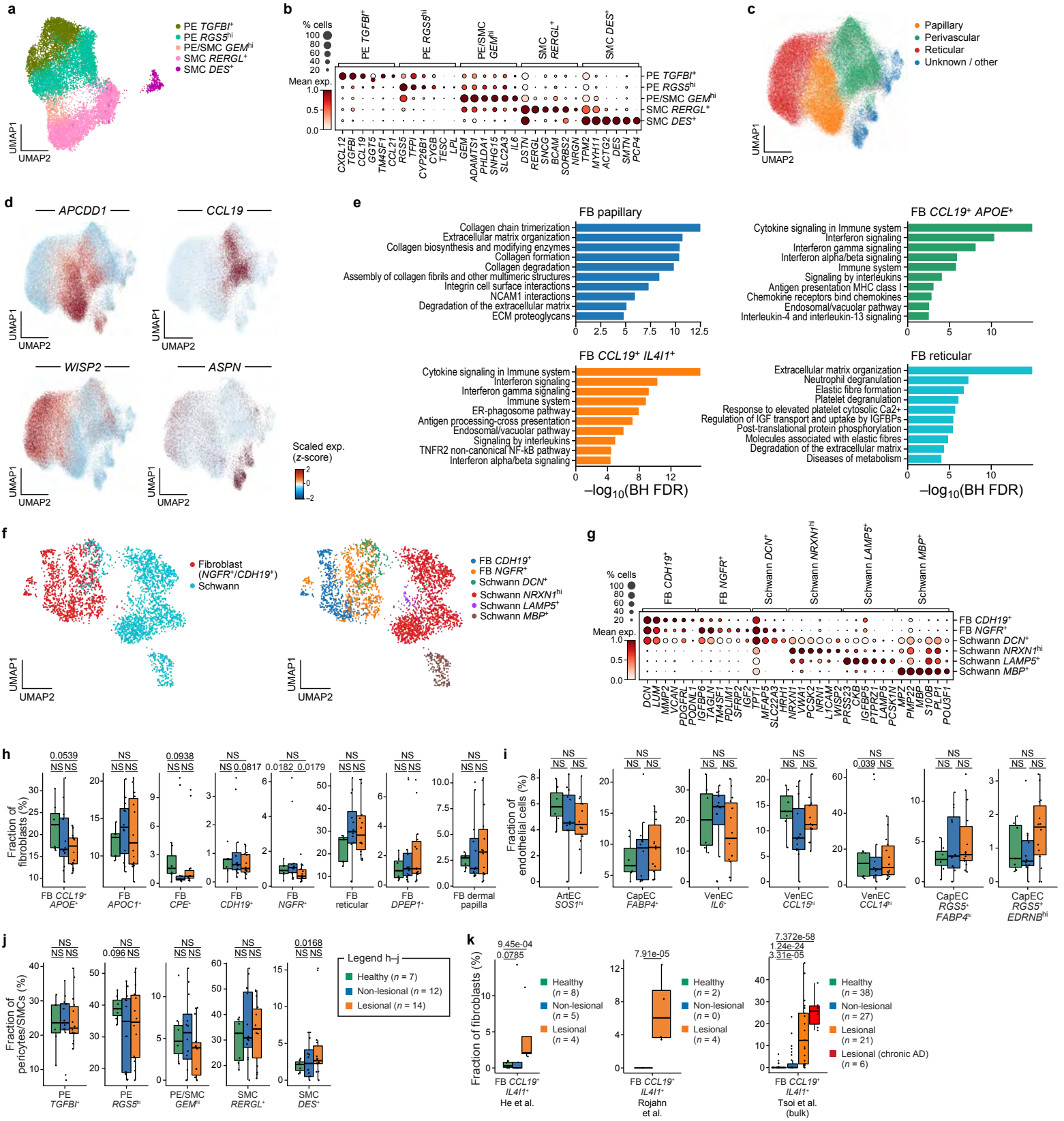
a
PE TGFBI+
PE RGS5hi
PE/SMC GEMhi
SMC RERGL+
SMC DES+
UMAP1
UMAP2
b
% cells
Mean exp.
PE TGFBI+
PE RGS5hi
PE/SMC GEMhi
SMC RERGL+
SMC DES+
CXCL12 TGFBI CCL19 GGT5 TM4SF1 CCL21 RGS5 TFPI CYP26B1 CYGB TESC LPL GEM ADAMTS1 PHLDA1 SNHG15 SLC2A3 IL6 DSTN RERGL SNCG BCAM SORBS2 NRGN TPM2 MYH11 ACTG2 DES SMTN PCP4
c
Papillary
Perivascular
Reticular
Unknown / other
UMAP1
UMAP2
d
APCDD1
CCL19
WISP2
ASPN
Scaled exp. (z-score)
UMAP1
UMAP2
e
FB papillary
Collagen chain trimerization
Extracellular matrix organization
Collagen biosynthesis and modifying enzymes
Collagen formation
Collagen degradation
Assembly of collagen fibrils and other multimeric structures
Integrin cell surface interactions
NCAM1 interactions
Degradation of the extracellular matrix
ECM proteoglycans
FB CCL19+ APOE+
Cytokine signaling in Immune system
Interferon signaling
Interferon gamma signaling
Interferon alpha/beta signaling
Immune system
Signaling by interleukins
Antigen presentation MHC class I
Chemokine receptors bind chemokines
Endosomal/vacuolar pathway
Interleukin-4 and interleukin-13 signaling
FB CCL19+ IL4I1+
Cytokine signaling in Immune system
Interferon signaling
Interferon gamma signaling
Immune system
ER-phagosome pathway
Antigen processing-cross presentation
Endosomal/vacuolar pathway
Signaling by interleukins
TNFR2 non-canonical NF-kB pathway
Interferon alpha/beta signaling
FB reticular
Extracellular matrix organization
Neutrophil degranulation
Elastic fibre formation
Platelet degranulation
Response to elevated platelet cytosolic Ca2+
Regulation of IGF transport and uptake by IGFBPs
Post-translational protein phosphorylation
Molecules associated with elastic fibres
Degradation of the extracellular matrix
Diseases of metabolism
–log10(BH FDR)
f
Fibroblast (NGFR+/CDH19+)
Schwann
FB CDH19+
FB NGFR+
Schwann DCN+
Schwann NRXN1hi
Schwann LAMP5+
Schwann MBP+
UMAP1
UMAP2
g
% cells
Mean exp.
FB CDH19+
FB NGFR+
Schwann DCN+
Schwann NRXN1hi
Schwann LAMP5+
Schwann MBP+
DCN LUM MMP2 VCAN PDGFRL PODNL1 IGFBP6 TAGLN TM4SF1 PDLIM1 SFRP2 IGF2 TPT1 MFAP5 SLC22A3 HRH1 NRXN1 VWA1 PCSK2 NRXN1 LYPD1 WISP3 PRSS23 CKB IGFBP5 PTPRZ1 LAMP5 PCSK1N MPZ PMP22 MBP S100B PLP1 POU3F1
h
Fraction of fibroblasts (%)
0.0539 NS NS
NS NS NS
0.0938 NS NS
NS NS 0.0817
0.0182 0.0179
NS NS NS
NS NS NS
NS NS NS
FB CCL19+ APOE+
FB APOC1+
FB CPE+
FB CDH19+
FB NGFR+
FB reticular
FB DPEP1+
FB dermal papilla
i
Fraction of endothelial cells (%)
NS NS NS
NS NS NS
NS NS NS
NS NS NS
NS 0.039 NS
NS NS NS
NS NS NS
ArtEC SOS1hi
CapEC FABP4+
VenEC IL6+
VenEC CCL15hi
VenEC CCL14hi
CapEC RGS5+ FABP4hi
CapEC RGS5+ EDRNBhi
j
Fraction of pericytes/SMCs (%)
NS NS NS
NS 0.096 NS
NS NS NS
NS NS NS
0.0168 NS NS
PE TGFBI+
PE RGS5hi
PE/SMC GEMhi
SMC RERGL+
SMC DES+
Legend h–j
Healthy (n = 7)
Non-lesional (n = 12)
Lesional (n = 14)
k
Fraction of fibroblasts (%)
9.45e-04
0.0785
7.91e-05
7.372e-58
1.24e-24
3.31e-05
Healthy (n = 8)
Non-lesional (n = 5)
Lesional (n = 4)
Healthy (n = 2)
Non-lesional (n = 0)
Lesional (n = 4)
Healthy (n = 38)
Non-lesional (n = 27)
Lesional (n = 21)
Lesional (chronic AD) (n = 6)
FB CCL19+ IL4I1+ He et al.
FB CCL19+ IL4I1+ Rojahn et al.
FB CCL19+ IL4I1+ Tsoi et al. (bulk)

Supplementary Figure 11. Stromal cell diversity in healthy and AD skin.

a,b, Pericyte and vascular smooth muscle cell (SMC) subsets. **a**, 2D embedding of scRNA-seq profiles of pericytes and SMCs from healthy and AD skin, colored by subset. **b**, Mean expression (dot color) and fraction of expressing cells (dot size) of pericyte and SMC subset marker genes (columns) across cell subsets (rows). **c,d**, Fibroblast subsets. 2D embedding of scRNA-seq profiles of fibroblasts from healthy and AD skin, colored by their proposed dermal location[110,111] (c) or by marker gene expression (d, z-score). **e**, Distinct functional processes in fibroblast subsets. Reactome[109] terms (rows) enriched (x axis, $-\log_{10}$(BH FDR), Fisher's exact test) in each fibroblast subset (**STAR Methods**). **f,g**, Schwann-like fibroblast subsets. **f**, 2D embedding of scRNA-seq profiles of Schwann-like fibroblasts and Schwann cells from healthy and AD skin, colored by coarse (left) or granular (right) subset. **g**, Mean expression (dot color) and proportion of expressing cells (dot size) of Schwann-like fibroblast and Schwann cell subset marker genes (columns) in each cell subset (rows). **h-j**, Cell subsets that are largely unchanged across conditions. Cell proportions (y axis) of different subsets of fibroblasts (h), endothelial cells (i) or pericyte/SMCs (j) across conditions (color). Lesional, n = 14 channels (9 samples), non-lesional, n = 12 channels (8 samples), healthy, n = 7 channels (6 samples). Center line: median; box limits: first and third quartiles; whiskers: 1.5× interquartile range. Dirichlet regression, ns: non-significant. Dots: cell type proportion by channel. **k**, Increased abundance of classified *CCL19*$^+$ *IL4I1*$^+$ fibroblasts in lesional AD skin across studies. Proportion (y axis) of *CCL19*$^+$ *IL4I1*$^+$ fibroblasts annotated by our classifier (**Methods**) in published scRNA-seq studies (k, left[8] and middle[11]) and deconvoluted bulk RNA-seq (k, right[19]). Dots: cell type proportion by sample.

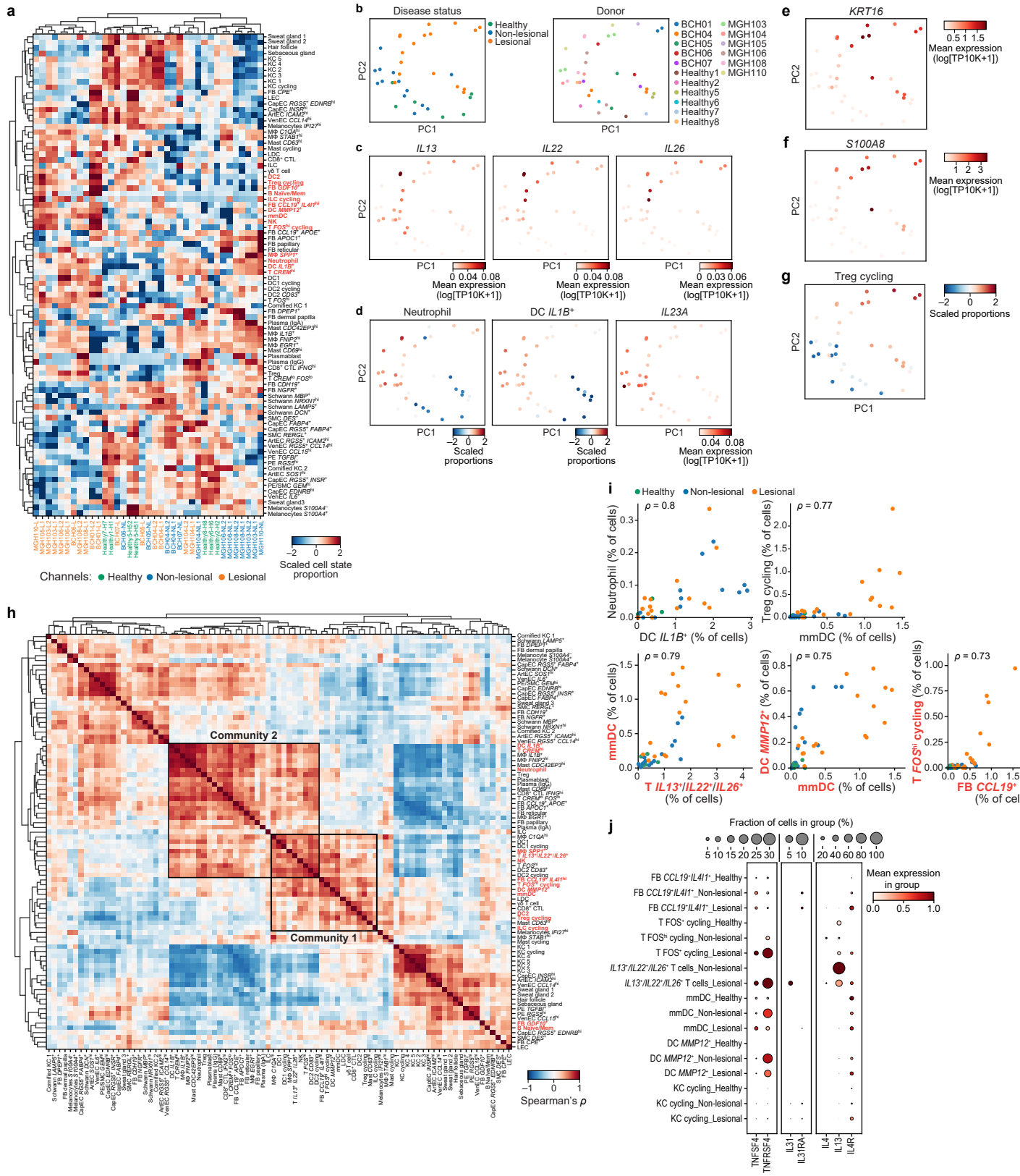
a
Channels: Healthy Non-lesional Lesional
Scaled cell state proportion
b
Disease status
Healthy
Non-lesional
Lesional
Donor
BCH01 BCH04 BCH05 BCH06 BCH07 Healthy1 Healthy2 Healthy5 Healthy6 Healthy7 Healthy8
MGH103 MGH104 MGH105 MGH106 MGH108 MGH110
PC1
PC2
c
IL13
IL22
IL26
Mean expression (log[TP10K+1])
d
Neutrophil
DC IL1B+
IL23A
Scaled proportions
e
KRT16
f
S100A8
g
Treg cycling
h
Community 2
Community 1
Spearman's ρ
i
Healthy Non-lesional Lesional
Neutrophil (% of cells)
DC IL1B+ (% of cells)
Treg cycling (% of cells)
mmDC (% of cells)
mmDC (% of cells)
T IL13+/IL22+/IL26+ (% of cells)
DC MMP12+ (% of cells)
mmDC (% of cells)
T FOSHi cycling (% of cells)
FB CCL19+ IL4I1+ (% of cells)
j
Fraction of cells in group (%)
Mean expression in group
FB CCL19+IL4I1+_Healthy
FB CCL19+IL4I1+_Non-lesional
FB CCL19+IL4I1+_Lesional
T FOS+ cycling_Healthy
T FOSHi cycling_Non-lesional
T FOS+ cycling_Lesional
IL13+/IL22+/IL26+ T cells_Non-lesional
IL13+/IL22+/IL26+ T cells_Lesional
mmDC_Healthy
mmDC_Non-lesional
mmDC_Lesional
DC MMP12+_Healthy
DC MMP12+_Non-lesional
DC MMP12+_Lesional
KC cycling_Healthy
KC cycling_Non-lesional
KC cycling_Lesional
TNFSF4 TNFRSF4
IL31 IL31RA
IL4 IL13 IL4R

Supplementary Figure 12. Multicellular communities in lesional AD skin.

a-g, Channel characterization by cell composition. **a**, Scaled proportions (z-scores of centered log ratio (CLR) transformed proportions, color) of granular cell subsets (rows) across channels (columns). Red: cell subsets with high PC2 loading (**Fig. 6b**). **b-g**, 2D embedding of healthy, non-lesional and lesional channels along the first two PCs from PCA of cell composition, colored by disease status (b, left), individual (b, right), mean expression of effector T cell cytokines (c) or epidermal inflammation markers (e and f) or scaled cell subset proportions (d and g). **h**, Correlation coefficient (Spearman's ρ, colorbar) between proportions of each pair of 86 granular cell subsets (rows, columns) across samples (larger version of **Fig. 6c**). Red: cell subsets with high PC2 loading. **i**, Selected correlated cell subsets from Community 1 and Community 2. Proportion of cells (x and y axis) of selected pairs of subsets in each channel from healthy (green), non-lesional (blue) or lesional (orange) skin. Top left: Spearman's ρ. **j**, Immune-signaling gene expression in AD drug-targeted pathways. Gene expression (dot color) is min-max scaled across genes, and the proportion of cells expressing the gene (dot size) is shown. Community 1 cell subsets and cycling KCs (rows) across disease status are highlighted.

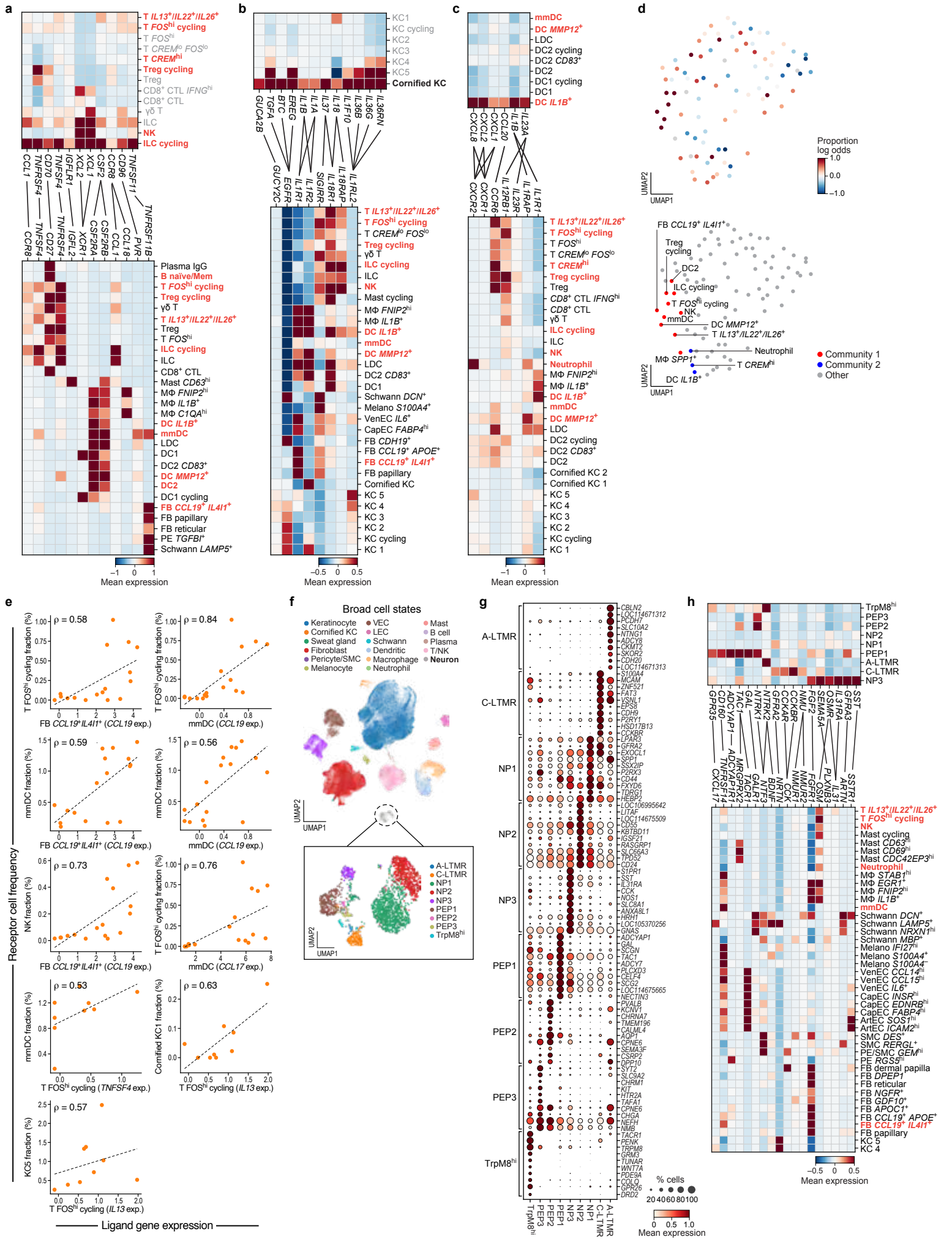
a
b
c
d
e
f
g
h
Mean expression
Proportion log odds
Community 1
Community 2
Other
Broad cell states
Keratinocyte
Cornified KC
Sweat gland
Fibroblast
Pericyte/SMC
Melanocyte
VEC
LEC
Schwann
Dendritic
Macrophage
Neutrophil
Mast
B cell
Plasma
T/NK
Neuron
A-LTMR
C-LTMR
NP1
NP2
NP3
PEP1
PEP2
PEP3
TrpM8hi
% cells
Receptor cell frequency
Ligand gene expression

Supplementary Figure 13. Cell-cell interactions in AD.

a-c, Cell-cell interactions formed by cycling ILCs, cornified KCs and *IL1B*$^{+}$ DCs. Mean z-scored expression values (color) of ligand and receptor genes of cycling ILCs (a), cornified KCs (b) or *IL1B*$^{+}$ DCs (c) across related cell subsets (top, rows) and their cognate interacting partners (bottom, columns) across all cell subsets with significant interacting partner expression (bottom, rows) (**Methods**). Lines: interacting ligand-receptor pairs. Red: cell subsets with high PC2 loading (**Fig. 6b**). **d**, Relation between cellular communities. 2D UMAP embedding of granular cell subset proportion profiles (dots) across all samples colored by proportion log odds (top) and community membership (bottom). Positive log odds: enriched in lesional. **e**, Correlation between ligand expression and proportion of cells expressing a cognate receptor in Community 1. Mean expression level of a ligand in one cell subset (x axis) and proportion of a cell subset expressing the cognate receptor (y axis) in each lesional channel. Dashed line: best linear fit. Top left: Spearman's ρ. **f-h**, Putative interactions with peripheral neurons. **f**, 2D embeddings of scRNA-seq profiles of all cells from the current study and from a published non-human primate dorsal root ganglion (DRG) scRNA-seq dataset[52] (top) (**Methods**), and from the DRG neurons only (bottom, inset), colored by cell types. **g**, Mean expression (dot color) and fraction of expressing cells (dot color) of peripheral neuron marker genes (columns) across cell subsets (rows). **h**, Mean expression (color, z-score) of neuron-specific ligand and receptor genes (left, rows) across DRG neuron subsets (left, columns) and of their cognate interacting genes (right, rows) in each skin cell subset with significant expression (right, columns). Lines: ligand-receptor pairs. Red: cell subsets with high PC2 loading (**Fig. 6b**).

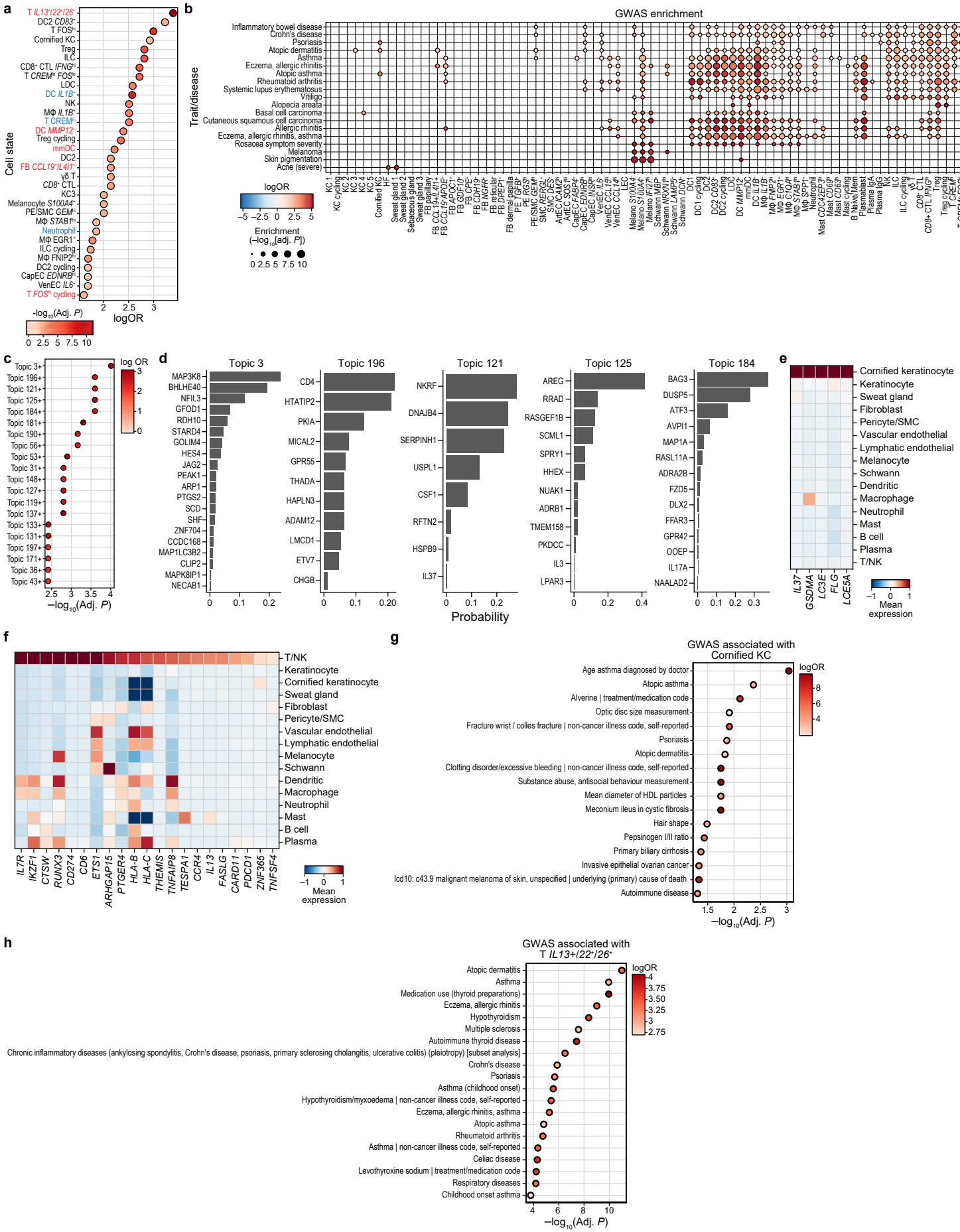
a
Cell state
logOR
-log10(Adj. P)
b
GWAS enrichment
Trait/disease
Inflammatory bowel disease
Crohn's disease
Psoriasis
Atopic dermatitis
Asthma
Eczema, allergic rhinitis
Atopic asthma
Rheumatoid arthritis
Systemic lupus erythematosus
Vitiligo
Alopecia areata
Basal cell carcinoma
Cutaneous squamous cell carcinoma
Allergic rhinitis
Eczema, allergic rhinitis, asthma
Rosacea symptom severity
Melanoma
Skin pigmentation
Acne (severe)
logOR
Enrichment
(–log10[adj. P])
c
log OR
–log10(Adj. P)
d
Topic 3
Topic 196
Topic 121
Topic 125
Topic 184
Probability
e
Cornified keratinocyte
Keratinocyte
Sweat gland
Fibroblast
Pericyte/SMC
Vascular endothelial
Lymphatic endothelial
Melanocyte
Schwann
Dendritic
Macrophage
Neutrophil
Mast
B cell
Plasma
T/NK
Mean expression
f
T/NK
Keratinocyte
Cornified keratinocyte
Sweat gland
Fibroblast
Pericyte/SMC
Vascular endothelial
Lymphatic endothelial
Melanocyte
Schwann
Dendritic
Macrophage
Neutrophil
Mast
B cell
Plasma
Mean expression
g
GWAS associated with
Cornified KC
logOR
Age asthma diagnosed by doctor
Atopic asthma
Alverine | treatment/medication code
Optic disc size measurement
Fracture wrist / colles fracture | non-cancer illness code, self-reported
Psoriasis
Atopic dermatitis
Clotting disorder/excessive bleeding | non-cancer illness code, self-reported
Substance abuse, antisocial behaviour measurement
Mean diameter of HDL particles
Meconium ileus in cystic fibrosis
Hair shape
Pepsinogen I/II ratio
Primary biliary cirrhosis
Invasive epithelial ovarian cancer
Icd10: c43.9 malignant melanoma of skin, unspecified | underlying (primary) cause of death
Autoimmune disease
–log10(Adj. P)
h
GWAS associated with
T IL13+/22+/26+
logOR
Atopic dermatitis
Asthma
Medication use (thyroid preparations)
Eczema, allergic rhinitis
Hypothyroidism
Multiple sclerosis
Autoimmune thyroid disease
Chronic inflammatory diseases (ankylosing spondylitis, Crohn's disease, psoriasis, primary sclerosing cholangitis, ulcerative colitis) (pleiotropy) [subset analysis]
Crohn's disease
Psoriasis
Asthma (childhood onset)
Hypothyroidism/myxoedema | non-cancer illness code, self-reported
Eczema, allergic rhinitis, asthma
Atopic asthma
Rheumatoid arthritis
Asthma | non-cancer illness code, self-reported
Celiac disease
Levothyroxine sodium | treatment/medication code
Respiratory diseases
Childhood onset asthma
–log10(Adj. P)

Supplementary Figure 14. GWAS gene enrichment in skin cell subsets.

a, *IL13*$^+$*/IL22*$^+$*/IL26*$^+$ T cells and cornified KCs are enriched in expression of AD GWAS genes. Skin cell subsets (rows) enriched (-log$_{10}$(FDR), Fisher's exact test, dot color) for expressing AD GWAS nominated genes, sorted by odds ratio (x axis, log$_2$ scale) (BH FDR < 0.05). Red: Cells from Community 1. Blue: Cells from Community 2. **b**, Relation of skin cell subsets to skin and inflammatory diseases. Enrichment (-log$_{10}$(FDR), Fisher's exact test, dot color) and odds ratio (log$_2$, dot size) of GWAS nominated gene sets for inflammatory and skin-related traits (rows) in genes expressed in each skin cell subset (columns) (**Methods**). **c,d**, Lymphocyte gene program enriched in AD GWAS genes. **c**, Topics (rows) enriched (-log$_{10}$(BH FDR), Fisher's exact test, x axis) for expressing AD GWAS nominated genes, sorted by -log$_{10}$(BH FDR) and colored by log odds ratio (BH FDR<0.05). **d**, Probabilities (y axis) of each of the top scoring genes (y axis) in each of the top five GWAS enriched topics (after topic 190) (**Methods**). **e,f**, Selected AD GWAS-nominated genes expressed in skin cell subsets. Mean expression (color, z-score) of cornified KC-specific (e) or lymphocyte-specific (f) AD GWAS genes (rows) in coarse cell types (rows). **g,h**, Enrichment of GWAS genes from various atopic and type 2 inflammatory diseases in cornified KCs and *IL13*$^+$*/IL22*$^+$*/IL26*$^+$ co-expressing T cells. Significance (-log$_{10}$(BH FDR), x axis) and effect size (log$_2$(odds ratio), dot color) of enrichment of GWAS nominated gene sets for different traits (rows) enriched in cornified KCs (g) or *IL13*$^+$*/IL22*$^+$*/IL26*$^+$ co-expressing T cells (h) (**Methods**).